ANALYSIS OF CLIMATE EFFECTS ON AGRICULTURAL SYSTEMS

WHITE PAPER

A Report From:
California Climate Change Center

Prepared By:
Andrew Paul Gutierrez, Luigi Ponti, C. K. Ellis, and Thibaud d'Oultremont
University of California, Berkeley

Arnold Schwarzenegger, *Governor*

February 2006
CEC-500-2005-188-SF

Acknowledgements

We acknowledge support from the California Energy Commission and Environmental Protection Agency and the California Agricultural Extension Service. We thank Mary Tyree and Dan Cayan for supplying the climate projection scenarios and Michael Hanemann and Guido Franco for their guidance and leadership.

Preface

The Public Interest Energy Research (PIER) Program supports public interest energy research and development that will help improve the quality of life in California by bringing environmentally safe, affordable, and reliable energy services and products to the marketplace.

The PIER Program, managed by the California Energy Commission (Energy Commission), annually awards up to $62 million to conduct the most promising public interest energy research by partnering with Research, Development, and Demonstration (RD&D) organizations, including individuals, businesses, utilities, and public or private research institutions.

PIER funding efforts are focused on the following RD&D program areas:

- Buildings End-Use Energy Efficiency
- Energy-Related Environmental Research
- Energy Systems Integration
- Environmentally Preferred Advanced Generation
- Industrial/Agricultural/Water End-Use Energy Efficiency
- Renewable Energy Technologies

The California Climate Change Center (CCCC) is sponsored by the PIER program and coordinated by its Energy-Related Environmental Research area. The Center is managed by the California Energy Commission, Scripps Institution of Oceanography at the University of California at San Diego, and the University of California at Berkeley. The Scripps Institution of Oceanography conducts and administers research on climate change detection, analysis, and modeling; and the University of California at Berkeley conducts and administers research on economic analyses and policy issues. The Center also supports the Global Climate Change Grant Program, which offers competitive solicitations for climate research.

The California Climate Change Center Report Series details ongoing Center-sponsored research. As interim project results, these reports receive minimal editing, and the information contained in these reports may change; authors should be contacted for the most recent project results. By providing ready access to this timely research, the Center seeks to inform the public and expand dissemination of climate change information; thereby leveraging collaborative efforts and increasing the benefits of this research to California's citizens, environment, and economy.

For more information on the PIER Program, please visit the Energy Commission's website www.energy.ca.gov/pier/ or contact the Energy Commission at (916) 654-5164.

Table of Contents

List of Figures

Abstract

- Species of plants and animals have specific requirements for growth, survival, and reproduction that determine their geographic distribution, abundance, and interactions with other species. This study reviewed commonly used growth indices and more recently developed weather-driven, physiologically based demographic models.
- Physiologically based models were used to simulate the effects of various climate warming scenarios in California on species dominance in alfalfa, pest range extension of pink bollworm in cotton, bloom dates and yield in olive, and the biological control of the invasive vine mealybug in grape and the noxious weed yellow starthistle. Geographic information systems (GIS) technology was used to map the predicted effects of weather on plant/pest interactions across the varied ecological zones of California.
- In contrast to annual crops that can be easily moved to new areas as regional favorableness changes, reestablishment of long-lived species (e.g., grape and olive) would be costly in terms of time and money.
- The models predict that the geographic range of the different species in each system would be differentially affected, and this would complicate crop production and pest management issues. The effects of climate warming would limit tree crops that require chilling to initiate flowering. Olive was used as an example to show how its range would contract in the southern part of the state due to lack of chilling, and in the northern part of its range due to severe low temperatures. The range of pests such as pink bollworm on cotton would increase into formerly inhospitable areas of the San Joaquin Valley, and their damage would increase in the current range. Similar predictions would also apply for economically important pests such as olive fly, Mediterranean fruit fly and others. The range of invasive weeds weed such as yellow starthistle would also increase in a northward direction. The effects of warming climate on biological control agents are more difficult to predict, because the biological complexity of the interactions preclude generality. Marginal analysis of field and simulation data provides a way of analyzing the trends in such interactions.
- This study identified two major deficiencies: (1) the need to develop physiologically based systems models of the major cropping systems to forecast the effects of climate change on crops and on the dynamics of extant and new exotic pest introductions, and (2) the need to expand weather-gathering data systems, especially the collection of solar radiation data.

1.0 Introduction

Pests may be organisms of any taxa (e.g., arthropods, fungi, plants, vertebrates) that cause annoyance, disease, discomfort, or economic loss to humans. Most of our pests are exotic invasive species that, given current estimates, cause in excess of $137 billion in economic losses in the United States annually (Pimentel et al. 2000). Losses in California are likely in the range of $25–$40 billion annually. In an ecological context, pests are merely filling evolved roles in ecosystems that may have been simplified, or disrupted through domestication, inputs of nutrients and toxic substances (pesticides), or by human mismanagement. In courts of law, pest outbreaks are often assumed to be acts of God, but considerable research has shown that pest outbreaks have important climatic bases that affect their geographic distribution and severity.

Climate has profound impacts on the dynamics of agricultural and natural (e.g., fisheries and forestry) ecosystems (Walther 2002), and yet the regulation at low levels of most species that feed on plants occurs largely unnoticed by humans (DeBach 1964). However, this delicate balance can be disrupted by climate change. Among the pioneering works on the effects of weather in entomology were those of Messenger (1964, 1968), while a recent review of climate change on plant diseases is that of Coakley et al. (1999). In their edited volume, Reddy and Hodges (2001) review many aspects of current thinking on the effects of climate change in agriculture. To examine the impact of climate change on agricultural systems requires a holistic approach, often using models of the biology and dynamics of interacting species as driven by weather and other factors. The models help explain how the species respond to extant weather; understanding that can then be extrapolated to examine the potential effects of climate change on their dynamics. Questions we might wish to examine are: (1) how climate change will affect the geographic range, phenology, survival, productivity, and damage by pests of economically important species in natural and managed systems, and (2) how natural and biological control systems that keep them in check will be affected. Unfortunately, the literature on field applications of these topics is sparse (see Gilbert et al. 1976; Gutierrez 2001).

1.1. Review of Relevant Biological Modeling Literature

In the nineteenth and twentieth centuries, time series plots of daily, weekly, or monthly temperature, rainfall, vapor-pressure deficit, and other variables were used to create graphs that characterized climate zones favorable to plant and animal species. This empirical approach did not include the physiological growth response of species to climatic factors.

An important innovation was to characterize the growth rates of species in response to abiotic variables including aspects of weather (Fitzpatrick and Nix 1970). For example, the normalized concave (i.e., humped) growth rate index of a species on temperature would predictably have lower and upper thresholds and an optimum for development. Similar functions could be developed for other abiotic variables such as moisture (i.e., vapor pressure deficit), soil PH and nutrient content, and other factors. Any of these factors may greatly influence the distribution and abundance of species and the combined effects can be summarized mathematically. For example, the overall favorableness of conditions for growth (*GI*), say to temperature (*TI*), nitrogen (*NI*), soil

water (*WI*), and other factors time *t* at coordinate location *i,j* is the product of the individual indices, each of which have values between 0 and 1 (eqn. 1).

$$0 \leq GI_{ij}(t) = TI_{ij}(t)xNI_{ij}(t)xWI_{ij}(t)... \leq 1 \qquad (1)$$

A location becomes increasingly marginal as $G_{ij}(t) \rightarrow 0$, and any factor may make the site unfavorable because of the compounding effects. The growth index approach is an application of two old ideas, namely *von Liebig's Law of the Minimum* (1840) and *Shelford's Law of the Minimum* (1931). This study focuses on the effects of temperature and in some cases, soil moisture.

Field data on the limits of favorableness of temperature and indirectly plant soil moisture on three common aphid pests is summarized in Figure 1 as bi-variate normal distributions of the average temperature (*TI*) and moisture (*MI*) indices during periods when aphid abundance was high (Gutierrez et al. 1974). Note that oat-apple aphid (*Rhopalosiphum padi*) thrives in cooler, wetter climes than, for example, the cowpea aphid (*Aphis craccivora*), which thrives in an intermediate range of conditions, or the corn aphid (*R. maidis*), which thrives in hot, drier conditions. In general, each species in an ecosystem has its own set of unique conditions for growth and development. The most favorable conditions for the species would be in the central part of the bi-variate distribution and decrease toward the margins.

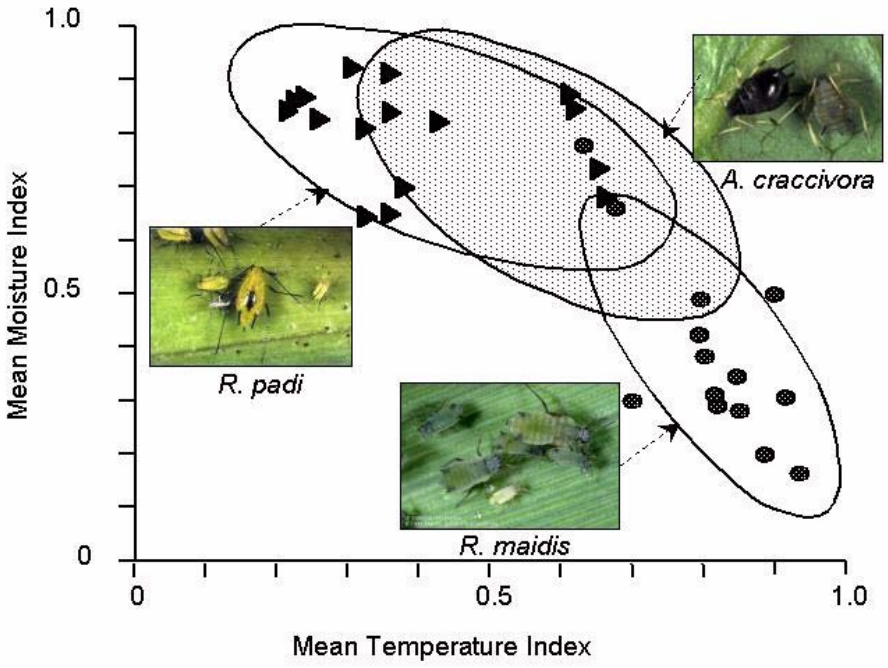

Figure 1. Bi-variate normal fits to indices of moisture and temperature of three exotic aphid pests (cf. Gutierrez et al. 1974; see also Sutherst et al. 1991).

In agriculture, agronomists through experimentation determine areas where specific crops grow best, but climate change could invalidate this knowledge. For example,

Figure 2a shows the tolerance indices to temperature (*TI*) and moisture (*MI*) for the interaction of three hypothetical species (i.e., a plant, its pest, and its natural enemy). The plant has a broad response to temperature and moisture levels; that of the herbivore is intermediate, and that of the predator is narrow. These limits would not be expected to change except on an evolutionary time scale. The dashed line in the figure is the average yearly pattern of *TI* and *MI* starting 1 January (i.e., the dot). The scenario in Figure 2a suggests a very good match of climate for the crop, while Figure 2b suggests moderate matching with increasing fall-winter-spring temperatures. Figure 2c depicts the effect of a large increase in rainfall. Such changes could readily occur due to climate change say in California. While the tolerances of the three species remain unchanged (say Figure 2a), climate change could make the area less favorable (e.g., Figure 2b–c) or possibly more favorable. The reality is that we are dealing with food webs, and climate change could affect these relationships and hence system structure and function.

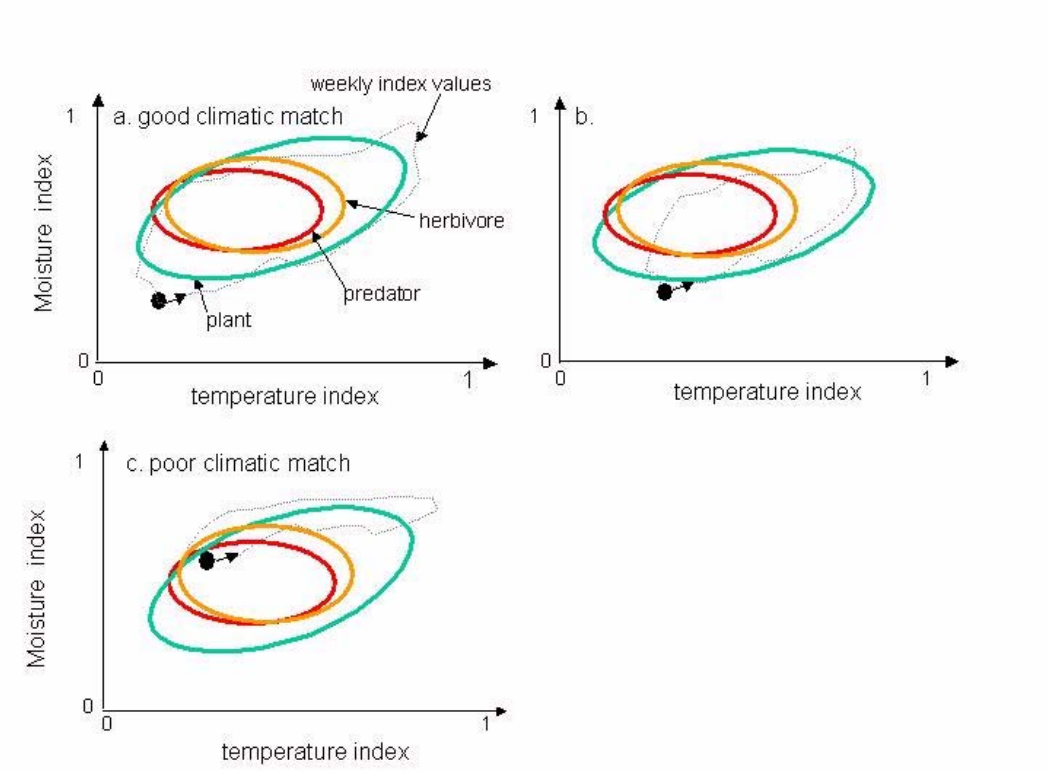

Figure 2. Climatic matching scenarios: (a) good, (b) moderate, and (c) poor. The yearly run of MI and TI values are depicted as the dashed line stating 1 January (i.e., ●).

The importance of temperature on the regulation of pests can be demonstrated using the case of the highly successful biological control of cottony cushion scale in citrus by the vedalia beetle (*Rodolia cardinalis*) and a parasitic fly (*Cryptochaetum iceryae*) (Quesada and DeBach 1973). This biological control program yielded hundreds of millions of dollars in benefit since 1887–1888 when the program was begun. The biology of the parasitic fly attacking this pest has a restricted range in cooler frost-free areas of California, while the vedalia beetle was able to control cottony cushion scale over a much wider area,

including the hotter areas of citrus production (Quesada and DeBach 1973). In another case, DeBach and Sundby (1963) showed that successive introductions of parasitoids to control California red scale on citrus resulted in a sequence of climatically better-adapted parasitoids displacing each other in some areas. This displacement occurred until each species established itself in the subset of Californian environments most favorable for its development. These and other biological control successes could be jeopardized by climate change. Climate change would also affect the distribution and severity of plant and animal diseases (e.g., Coakley et al. 1999).

1.2. Physiologically Based Dynamic Modeling

To understand how weather affects the dynamics of interacting plant and animal species, we must model the processes of growth, development, reproduction, and behavior of the species as driven by weather and other species in a general way—the model must be independent of time and place. Physiologically based demographic models of species that capture these processes have been developed (e.g., Gutierrez 1992, 1996; Gutierrez et al. 1975, 2005) and have early roots in the pioneering plant physiology modeling work of de Wit and Goudriaan (1978). Weather variables used to drive such models include daily max-min temperature, solar radiation, rainfall, run of wind, and relative humidity (RH). Development of models for the analysis of plant diseases may require additional inputs such as humidity, rainfall, and/or leaf wetness and other factors. The models may need to include important aspects of the biology such as the capacity of some species to enter dormancy during periods of extreme temperature and/or moisture stress often linked to photoperiod stimuli. Dormancy can have a strong influence on the yearly phenology of plant and animal species (e.g., Nechols et al. 1998), and even determine if a species can survive in an area. Models that capture these and other aspects of the biology can be used to make predictions about the biological systems across weather patterns and ecological conditions found in large landscapes such as California; predictions that can be mapped using geographic information systems (GIS) technology. The mathematics of the models used is summarized in Appendix A, and the papers cited therein.

This study used physiologically based models to examine the effects of observed weather and climate change scenarios on several agricultural systems. Researchers used historical weather for 105 locations in California for the period 1995–2005 (UC/IPM Program, www.ipm.ucdavis.edu/) to develop and test the models and to make predictions of crop-pest-natural enemy interactions, given current conditions as well as assumptions about climate change. To capture a range of uncertainty among climate models, two state-of-the-art global climate models (PCM and GFDLM) that capture a range of climate sensitivities were used in our analysis:

1. The Parallel Climate Model (PCM) from the National Center for Atmospheric Research (NCAR) and the U.S. Department of Energy (DOE) groups is a low-sensitivity model, with a climate sensitivity of approximately 1.8°C (3.2°F).
2. The Geophysical Fluids Dynamic Laboratory (GFDL) (NOAA Geophysical Dynamics Laboratory, Princeton New Jersey) model (Delworth et al. 2005), is a medium-sensitivity model with climate sensitivity of approximately 3°C (5.4°F).

The scenarios for daily weather for the period 1950–2100 based on assumptions about CO_2 levels were generated using the two global climate change models (i.e., with scenarios GFDLB1, GFDLA2, PCMB1, and PCMA2; see Hayhoe et al. 2004; Maurer 2005; Maurer and Duffy 2005) (see http://meteora.ucsd.edu/cap/cccc_model.html). Solar radiation data were not available from the climate models, hence the values were estimated from regressions of observed daily solar radiation on the difference of observed daily maximum and minimum temperatures. Seven locations on a north-south transect down the Great Central Valley of California (Red Bluff, Redding, Davis, Colusa, Fresno, Bakersfield, and Brawley in the extreme south) were selected to illustrate the effects of climate change on olive/olive fly interactions and yellow starthistle dynamics.

2.0 The Effects of Climate Warming on Crops and Pests

2.1. Alfalfa/Alfalfa Pests – Weather Effects on Species Dominance

There are roughly 1500 species of arthropod species in alfalfa, but few cause economic damage because they are under good natural control. A series of exotic pest have invaded alfalfa and have been largely controlled by introduced exotic natural enemies, as shown in Figure 3. Among the introduced pests are the pea aphid (*Acyrthosiphon pisum* (symbol *P*)) and blue alfalfa (*A. kondoi* (symbol *B*)) that initially caused great harm to alfalfa production in California (*A*) as they overwhelmed the capacity of native coccinellids (C) to control them. Two parasitoids (*Aphidius smithi* (*S*) and *A. ervi* (*E*)) and a fungal pathogen of the aphids, *Pandora neoaphidis* (*F),* were introduced in a biological control effort resulting in successful control across California and neighboring states. The parasitoid *A. smithi* is specific to pea aphid and is also ten times more susceptible to the fungal pathogen than is the blue aphid (Pickering and Gutierrez 1991). The sequence of introductions and species dominance were explored using assembly diagrams for dry and wet winter scenarios respectively (cf. Schreiber and Gutierrez 1998). The directional arrows indicate time and the symbols and the dashed arrows indicate when the different species entered the system.

During the normally wet Northern Californian winter, the pathogen causes catastrophic mortality to pea aphid (Pickering and Gutierrez 1991). However, during hot dry period periods, pathogen abundance declines and pea aphid may out-compete blue aphid.

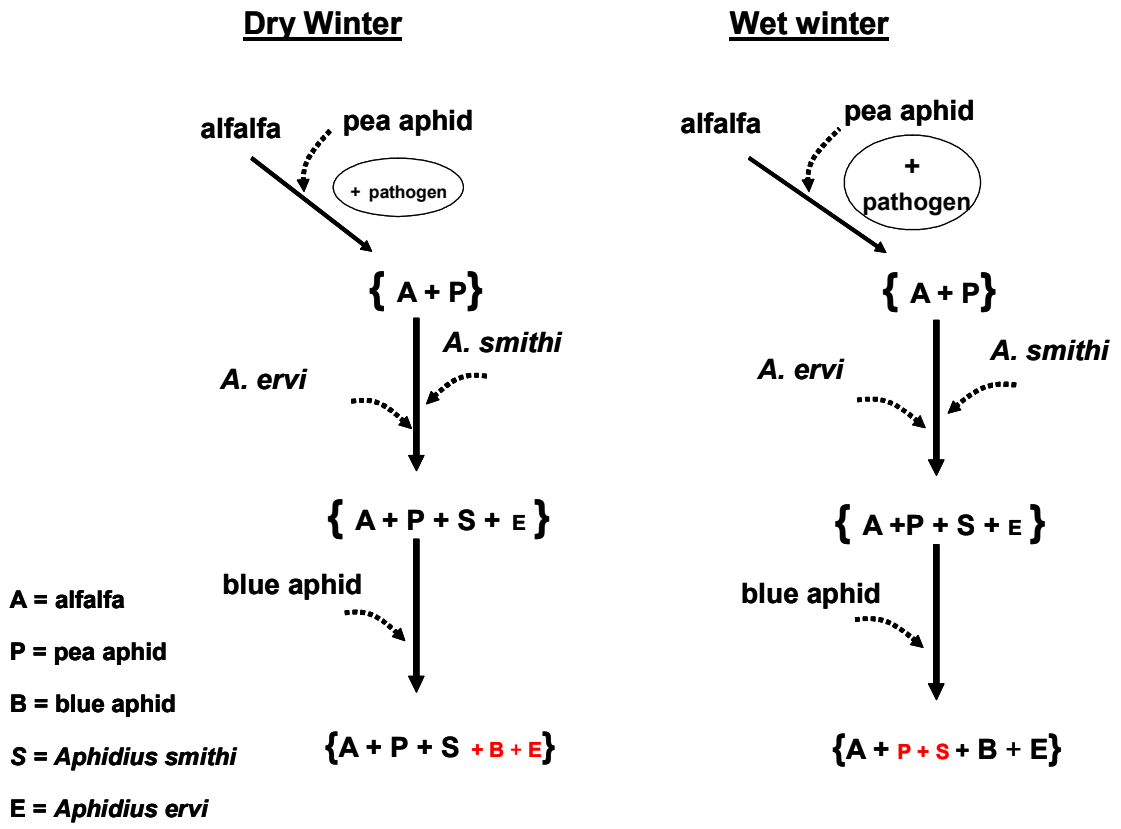

Figure 3. Assembly diagrams (sequence of introduction) for pea and blue aphids and their natural enemies in California alfalfa and the subsequent dominance of different species under dry and wet winters (see text for an explanation).

During dry winters, species A, P, and S dominate (i.e., the larger darker symbols), but during wet winters species A, B, and E dominate. The key point is that if climate change occurs, it may upset the balance between species in the food webs leading to new webs in this and other systems in unforeseen ways. In addition, new geographic distributions of species and increased (or decreased) pest numbers and impact may occur.

2.2. Grape/Vine Mealybug – Geographic Distribution and Relative Abundance

European grape vine is more tolerant of cold than is olive (see below), but climate change could affect not only yield but also the quality of the grapes and the wine produced from them. A recent invasive pest of grape, the vine mealybug (VMB, *Planococcus ficus*), has spread throughout many of California's grape-producing areas. Extensive biological control efforts are underway to control VMB, but to date success has been elusive. Complicating the problem is that the introduced natural enemies have very different tolerances to temperature (Gutierrez and Daane 2005). A physiologically based model of grape, VMB, and its natural enemies was used to examine their distribution and abundance as affected by extant weather at 105 locations in California over the period 1995–2004. The results for each season were mapped using GIS, and Figure 4 presents the results for 2004.

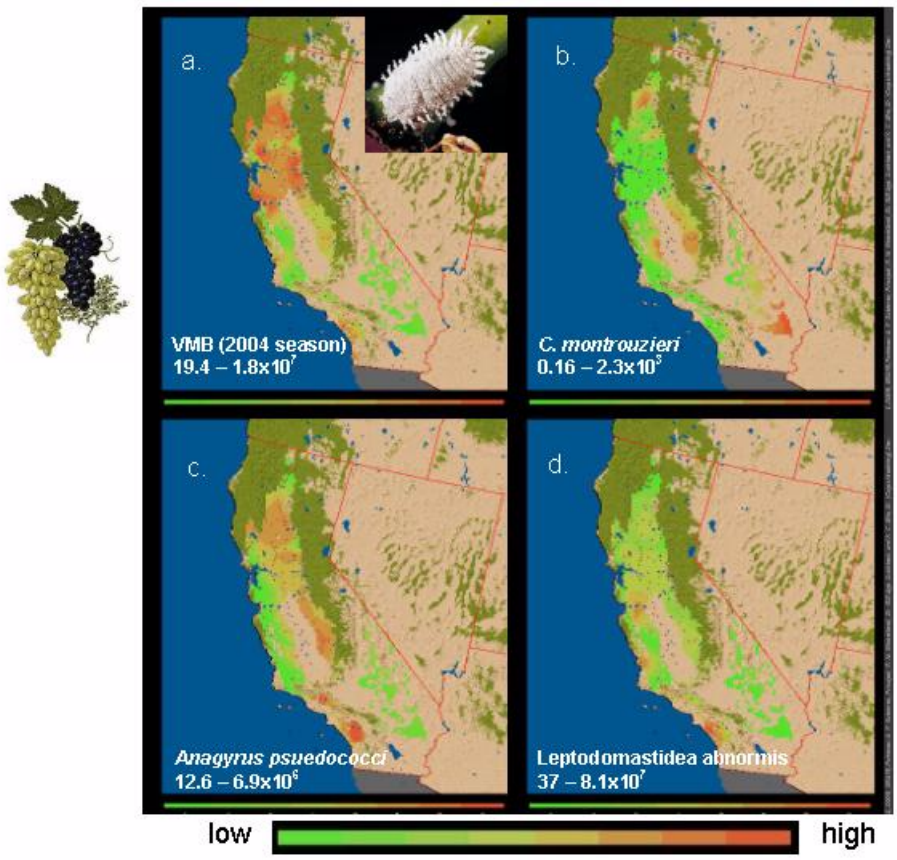

Figure 4. Predicted areas of favorableness (red = high for cumulative: (a.) mobile life stages of vine mealybug, (b.) predatory stages of the coccinelid predator *Crytolaemus montrouzieri* and two of introduced parasitoids, (c.) *Anagyrus psuedococci*, and (d.) *Leptomastidae abnormis*). Simulations are for the 2003 season in California Irrigation Management Information System (CIMIS) evapo-transpiration zones 3, 5, 6, 8, 10, 12, and 14.

Figure 4 shows the expected areas where VMB and each of the natural enemies would be most abundant (season-long cumulative values) after nine years of continuous simulation. High VMB densities occur in more northern regions and in coastal regions of southern California. VMB is less abundant in dryer warmer regions. The distribution and abundance of the natural enemies is patchy across the different grape growing regions. If biological control of VMB occurs, climate change could adversely affect it. Another invasive pest of grape is the glassy-winged sharpshooter, and it too is amenable to this kind of modeling and analysis.

2.3. Cotton/Pink Bollworm (PBW)

Cotton is grown as an annual in California throughout the southern half of the great Central Valley (i.e., the San Joaquin Valley) and the desert Valleys of southern California favorable climatically and economically for its production (see insert in Figure 5). Increasing temperatures in California could increase the potential range for cotton production further north into the Sacramento Valley. This section examines the effects of

climate change on pink bollworm (*Pectinophora gossypiella*, PBW), a major pest of California cotton.

Pink bollworm is a major pest of cotton worldwide, but its geographic range is limited by winter frosts that kill over-wintering dormant larvae. Venette et al. (2000) used the commercial software (CLIMEX, see Sutherst et al. 1991) to examine the potential range of PBW in the cotton-growing regions of the United States. Important limitations of the growth index approach such as CLIMEX are: the temporal dynamics and biology of the crop or the pest as driven by weather data, and often the only weather data used in the analysis are averages on different time scales. Venette et al. (2000) concluded that abiotic factors did not preclude the establishment of PBW over much of the cotton-growing regions of the United States. Gutierrez et al. (in press) used a physiologically based model of cotton growth and development and pink bollworm dynamics to examine the distribution of PBW in California on a finer scale. Multiyear simulations of the cotton–PBW system using historical weather data were run at each of 123 sites across Arizona and California, and a GIS was used to map the output data. Three different climate-warming scenarios were used to assess the potential distribution of PBW.

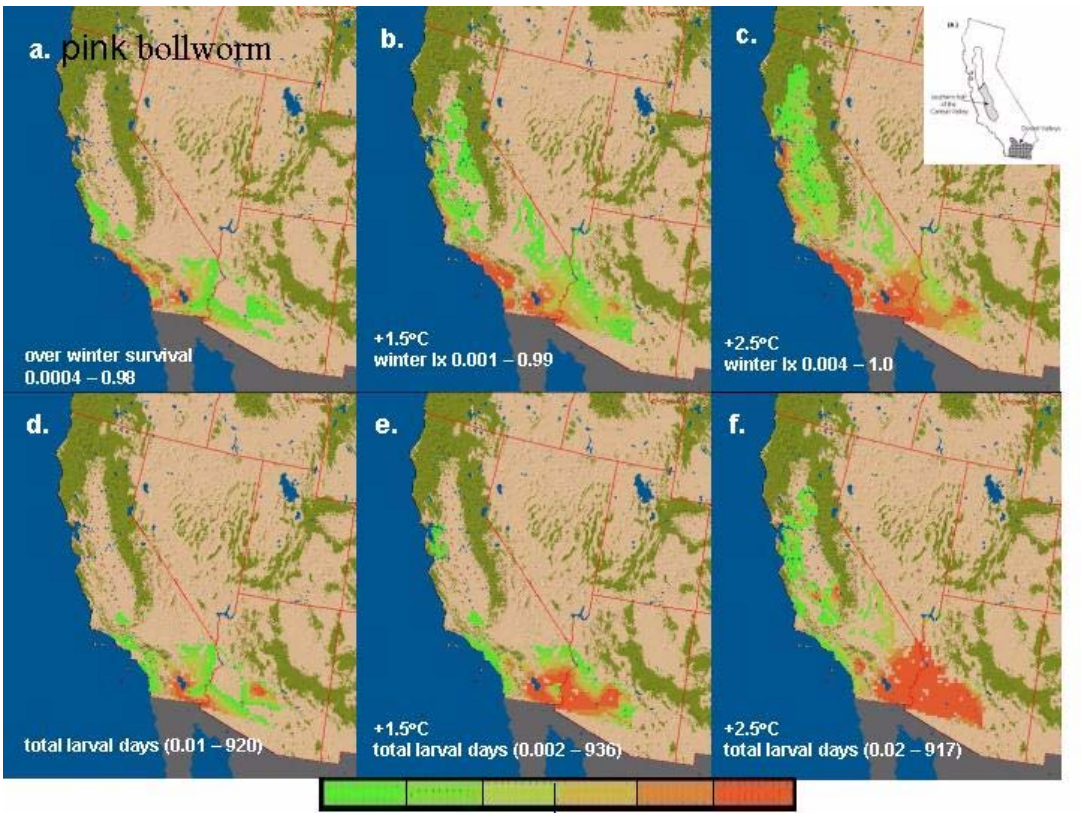

Figure 5. Cotton/pink bollworm: Predicting areas of favorableness. The effects on winter survival (a–c) and total seasonal pest PBW larval densities (larval days, d–e) under current weather (a, d) and with 1.5ºC or 2.7ºF (b, e) and 2.5ºC or 4.5ºF (c, f) increases in daily temperatures respectively (Gutierrez et al., in press). The inset figure indicates where cotton is currently grown, and the simulation results are for 2004.

The model predicts that PBW's range is currently restricted to the southern desert valleys of California (e.g., the Imperial and Coachella valleys and along the Colorado River) (Figure 5a, d; survival and cumulative larval days respectively). Winter frosts restrict PBW's invasion of the large cotton growing area of in the San Joaquin Valley (e.g. Gutierrez et al. 1977; in press). However, increasing temperatures, say 1.5°C–2.5°C (2.7°F–4.5°F), would greatly increase winter survival and extend the range of this pest northward into the San Joaquin Valley (Gutierrez et al., in press, Figure 5b, c, e, f). Furthermore, damage levels would increase in PBW's current range in the southern desert valleys of California and in Arizona.

2.4. Olive/Olive Fly

Olive is a drought-tolerant, long-lived plant with a distribution limited primarily by temperature. Like most temperate climate fruit trees (e.g., pome and stone fruits), olive requires winter chilling (i.e., vernalization) to stimulate fruit bud production and blooming (see Hartmann and Opitz 1980). In more tropical areas olive may grow without producing fruit. Among the approaches used to forecast olive chilling requirements for dormancy release and flowering have been artificial neural networks (Mancuso et al. 2002) and thermal summing (DeMelo-Abreu et al. 2004, eqn. 1 on page 119). This study used the latter approach and assumes that on average 450 hours chilling below a threshold of 7.3°C (45°F) are required for vernalization and 500 degree-days (dd) above the threshold are required for flowering.

Freezing temperatures may limit the distribution of olive culture. Denney and McEachern (1985; see also Dalla Marta et al. 2004) reviewed this literature and proposed a damage index model (I_d, eqn. 2, from page 230) for assessing the effects of the frequency of low (and high) temperatures during critical periods on damage to olive and its potential geographic distribution.

$$I_d = f_{SD} + 2f_K + 0.5f_{SF} + 0.25f_{HD} \qquad (2)$$

The weights represent the severity of the following effects,

f_{SD} = the number of days with temperature $\leq$ –8.3°C (17°F) (i.e., light damage),

f_K = days with temperature $\leq$ –12.2°C (10°F) (killing damage),

f_{SF} = days with $\leq$ 0°C ($\leq$ 32°F)after the beginning of max temperatures $\geq$ 21°C (70°F) (non-killing frost),

f_{HD} = days with temperatures $\geq$ 37.8°C ($\geq$ 100°F) during April or May (during the bloom period).

Cumulative daily damage indices for each year were computed using the four climate change scenarios at seven locations in the Great Central Valley. An arbitrary value of 40 *dd* below 0°C (32°F) was used to determine when olive trees are killed by cold. Some consequences of extant weather and of global warming scenarios on olive/olive fly dynamics are investigated below.

2.4.1. Olive model/GIS mapping

A physiologically based model of olive growth was used to assess the effects of extant weather on olive production and potential distribution in California (California Irrigation Management System evapo-transpiration zones 3, 5, 6, 8 , 10, and 14). The latest bloom dates and the highest yields are indicated by red, and the earliest bloom dates and lowest yields are indicated by green.

The predicted distribution of favorableness accords well with areas of olive culture in California (Figure 6). Spring frosts reduce yield, and/or freezing temperatures kill olive trees, limiting olive's northern range in the Great Central Valley. In contrast, lack of "chilling" and high-temperatures during blooming reduces fruit production in some areas (e.g., the southern desert regions of California).

Figure 6. Simulated bloom dates and yield (grams/tree) during 2003 in California Irrigation Management Information System (CIMIS) evapo-transpiration zones 3, 5, 6, 8, 10, 12, and 14.

2.4.2. Simulation of olive growth and development using the 150-year GFDL weather scenario.

The GFDLB1 scenario - We first use the medium-sensitivity GFDLB1 scenario with a climate sensitivity of approximately 3°C. Model output for Davis, Califonria, over 150

years shows that season length increases but with increasing variability (Figure 7a); the frequency of spring frost deceases (7b); bloom dates are earlier (7c); and predicted yields decline (31g per year) even in the absence of olive fly (i.e., with good pest control) due to increased plant respiration with temperature (7d). With olive fly infestations and in the absence of pest control, yields at Davis are low during the first 120 years and then begin to increase (7e vs. 7d) as increasing temperatures make the area increasingly unfavorable for olive fly (7f) (i.e., poor climate matching for the fly).

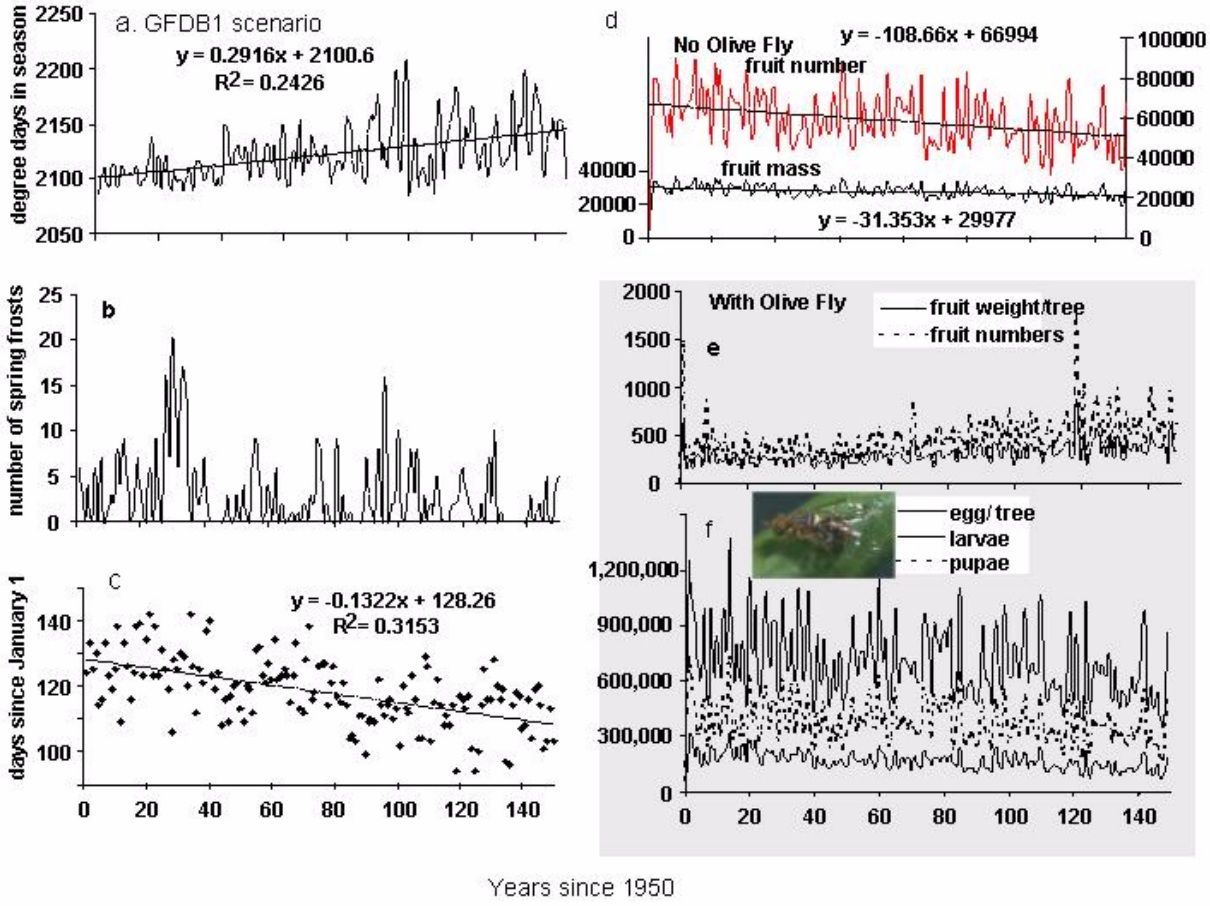

Figure 7. Simulations of olive using the 150 year GFDLB1 weather scenario: (a) season length, (b) spring frost days, (c) days to olive bloom, (d) olive fruit number and mass w/out olive fly, as well as with olive fly infestations, (e) olive fruit number and mass with olive fly, and (f) olive fly eggs, larvae, and pupae.

The GFDLA2 scenario - Using the GFDLA2 scenario for projected weather at Davis, California, (Figure 8a), the degree-days during the seasons increase at a faster rate than using the GFDLB1 scenario, and the number of spring frosts also decrease (Figure 8b). Tradeoffs between these two variables slow the time to bloom date (Figure 8c, 0.086 days per year) because vernalization of olive is delayed. Yields decrease in the absence of olive fly due to increasing respiration costs (see Figure 7). With uncontrolled olive fly infestations (Figure 8f), yields are severely depressed (Figure 8e) but increase to near

normal levels after year 125 (i.e., year 2075) but with greatly increased variability. Yield increases are due to decreased favorableness for olive fly due to high temperatures close to its climatic limits.

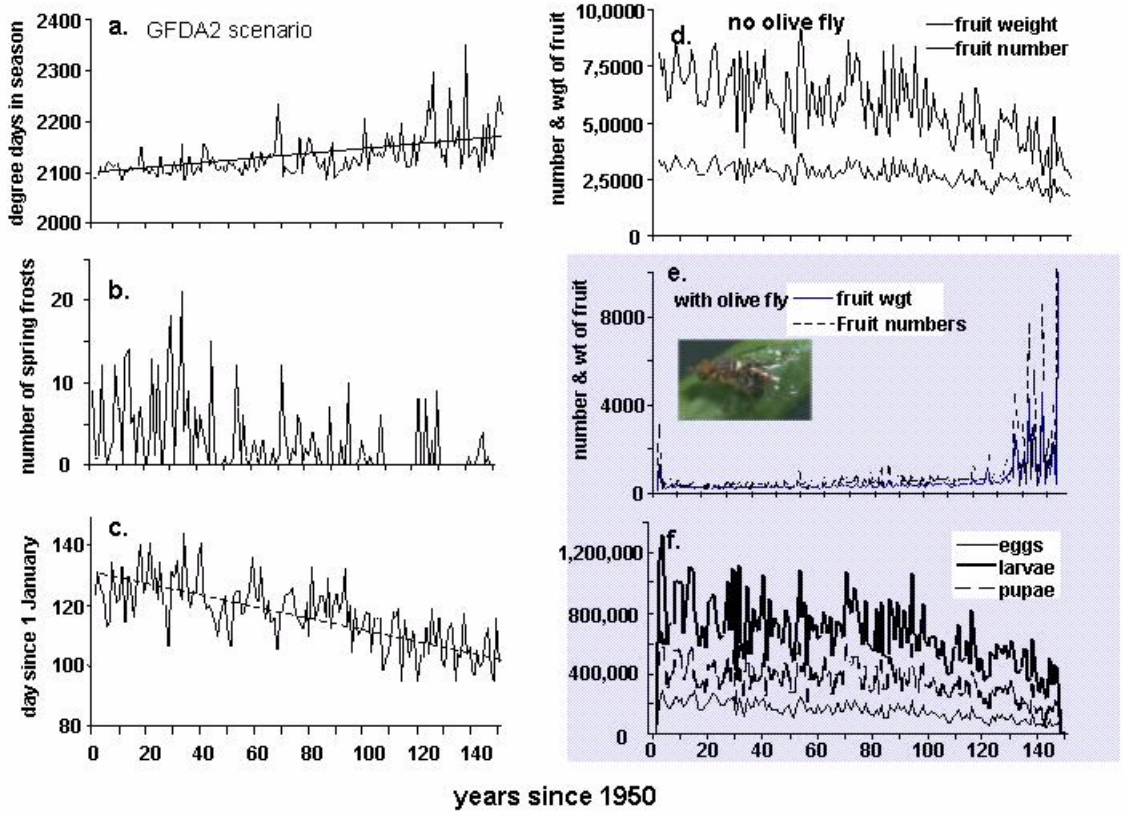

Figure 8. Simulations of olive using the 150-year GFDA2 weather scenario: (a) season length, (b) spring frost days, (c) days to olive bloom, (d) olive fruit number and mass w/out olive fly, as well as with olive fly infestations, (e) olive fruit number and mass with olive fly, and (f) olive fly eggs, larvae, and pupae.

2.4.3. Comparing climate change scenarios (PCMB1, PCMA2, GFDLB1, GFDLA2) for olive culture at seven locations

Seven locations on a north-south transect down the middle of the Great Central Valley of California were selected to compare time to bloom and the severity of yearly cumulative temperature damage indices to both low and high temperatures using four climate change scenarios.

PCMB1 scenario - Conditions are favorable for olive culture at all locations except Brawley in the very south of California, where vernalization requirements were infrequently met. The cumulative yearly damage indices (eqn. 2) due to low or high temperatures are low at Brawley and highest with high variable at Redding (Figure 9). Similarly, the time to bloom is longest at Redding, declining with decreasing latitude and being shortest at Bakersfield (roughly day 115 in year 1950 and day 105 in year 2100).

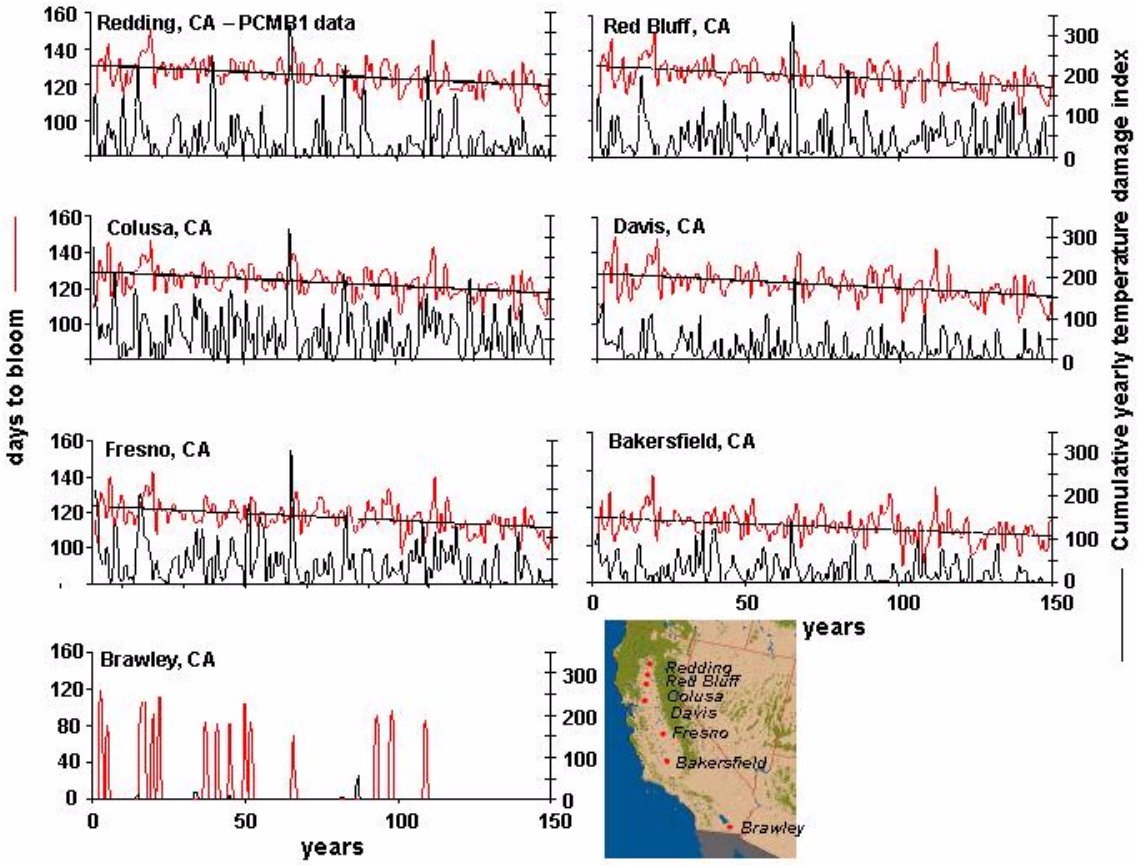

Figure 9. Simulations of olive using the 150-year PCMB1 weather scenario to predict days to olive bloom and cumulative temperature damage index at seven locations (see map insert).

PCMA2 scenario - Conditions are favorable for olive at all locations except Brawley in the very south of California and at Colusa north of Sacramento (Figure 10). Vernalization requirements were met infrequently at Brawley (i.e., the spikes, bloom date generally < 100 days since January 1), while predicted killing frosts occurred (i.e., threshold of 40 *dd* below 0°C, or 32°F) at Colusa, terminating olive culture there. The cumulative yearly temperature damage indices due to low or high temperatures are lowest at Brawley and highest at Redding and Colusa. The time to bloom is longest at Redding, declining with decreasing latitude and being shortest at Bakersfield.

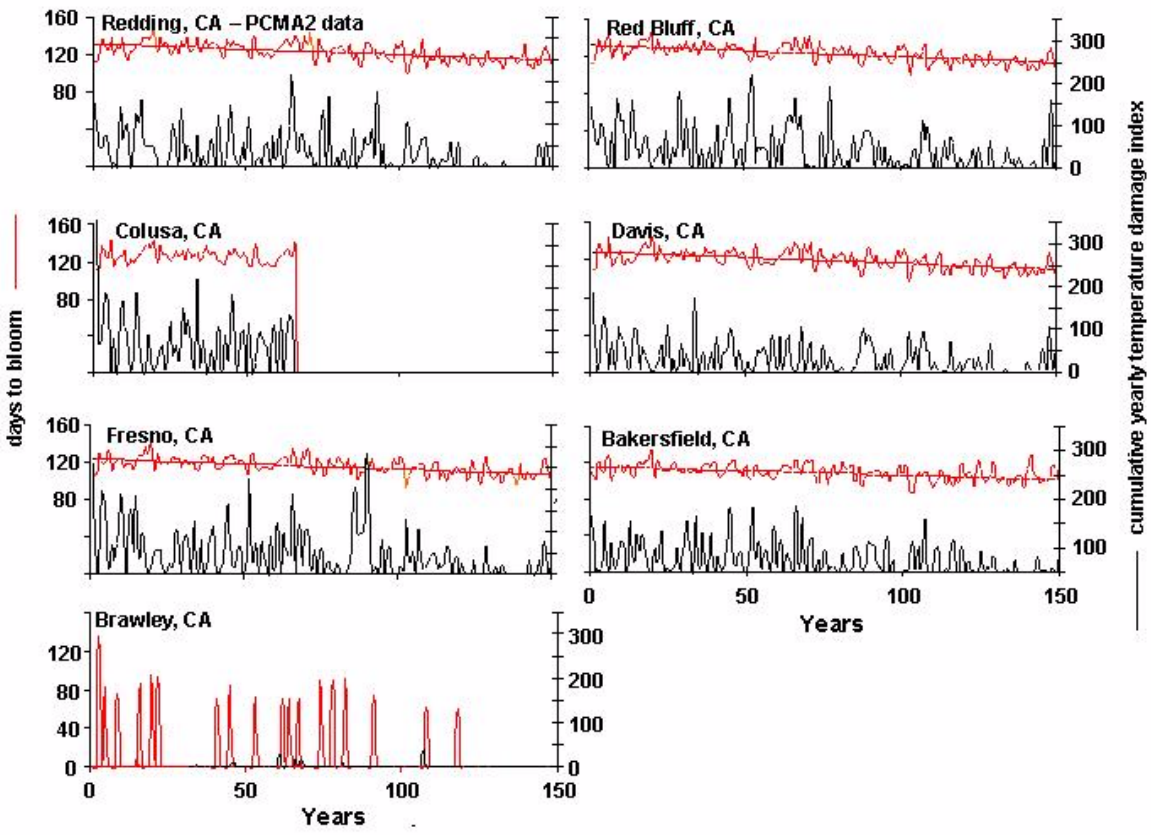

Figure 10. Simulations of olive, using the 150-year PCMA2 weather scenario to predict days to bloom and cumulative temperature damage index at seven locations.

GFDLB1 - Using the GFDLB1 scenario, conditions are favorable for olive at all locations except Brawley because of unmet vernalization requirements, and Colusa and Red Bluff, where heavy killing frosts are predicted (Figure 11). Cumulative yearly damage indices are low at Brawley and high at Redding (approximately 150), and are extremely high at Colusa (> 300). Olive growth ceased due to killing frosts at Red Bluff and Colusa (see Figure 13 below). In favorable areas, the times to bloom are longer at Redding but decline with decreasing latitude, being shortest at Bakersfield.

Subsequent runs eliminated the effects of killing frosts, to examine the favorableness for olive culture during the latter half of the climate-warming scenario (i.e., Figure 13 below).

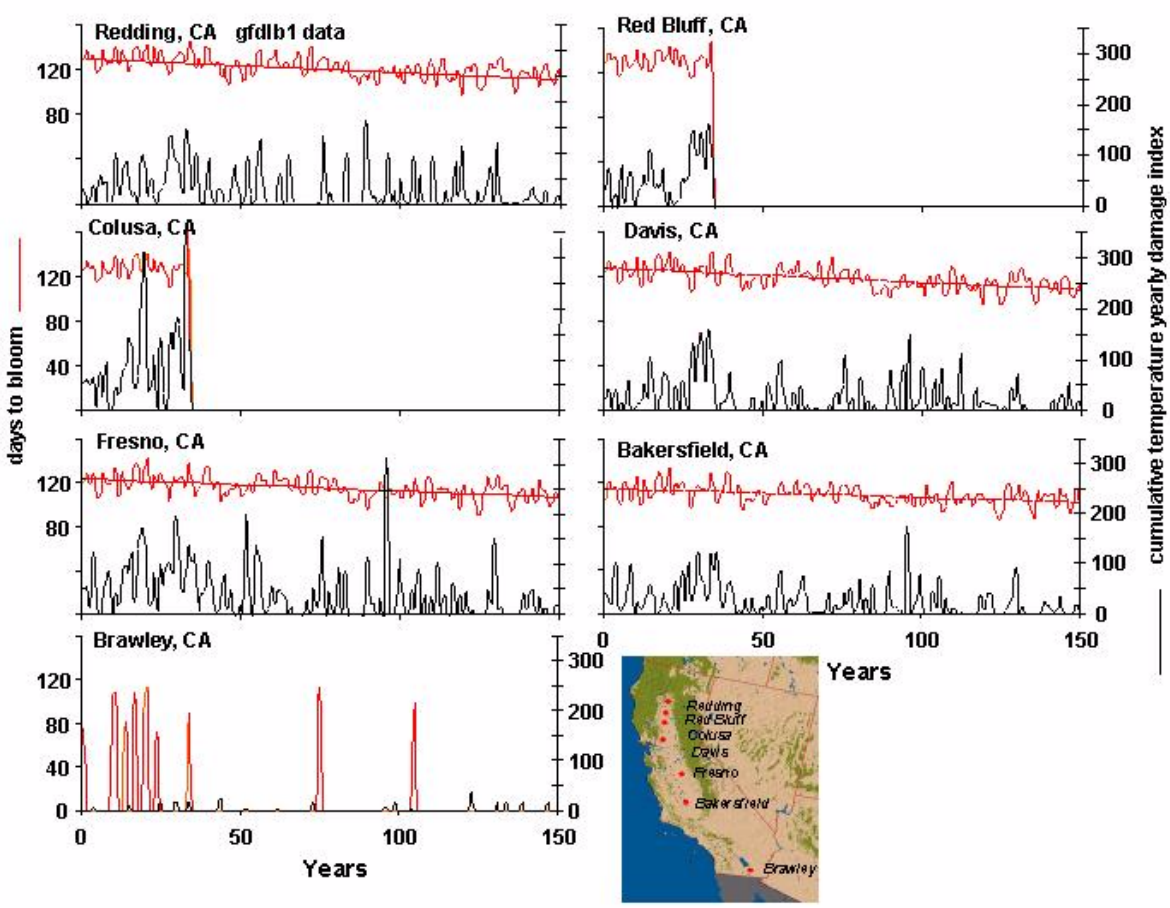

Figure 11. Simulations of olive, using the 150 years GFDLB1 weather scenario to predict days to bloom and cumulative temperature damage index at seven locations.

GFDLA2 – Using the GFDLA2 scenario, conditions are favorable for olives only in the central part of the Great Central Valley (Davis, Fresno, and Bakersfield) and unfavorable in the northern locations (Redding, Red Bluff, and Colusa) because of cold, and at Brawley, in southern California, where vernalization requirements were infrequently met (Figure 12). As in the other scenarios, climate warming increases favorableness for olive culture during later years of the run. In the locations favorable for olive growth, the cumulative yearly damage indices were lowest at Brawley, and highest at Fresno. The time to bloom decreases with latitude being shortest at Bakersfield. Note that failure to bloom increased in later years of the Bakersfield run.

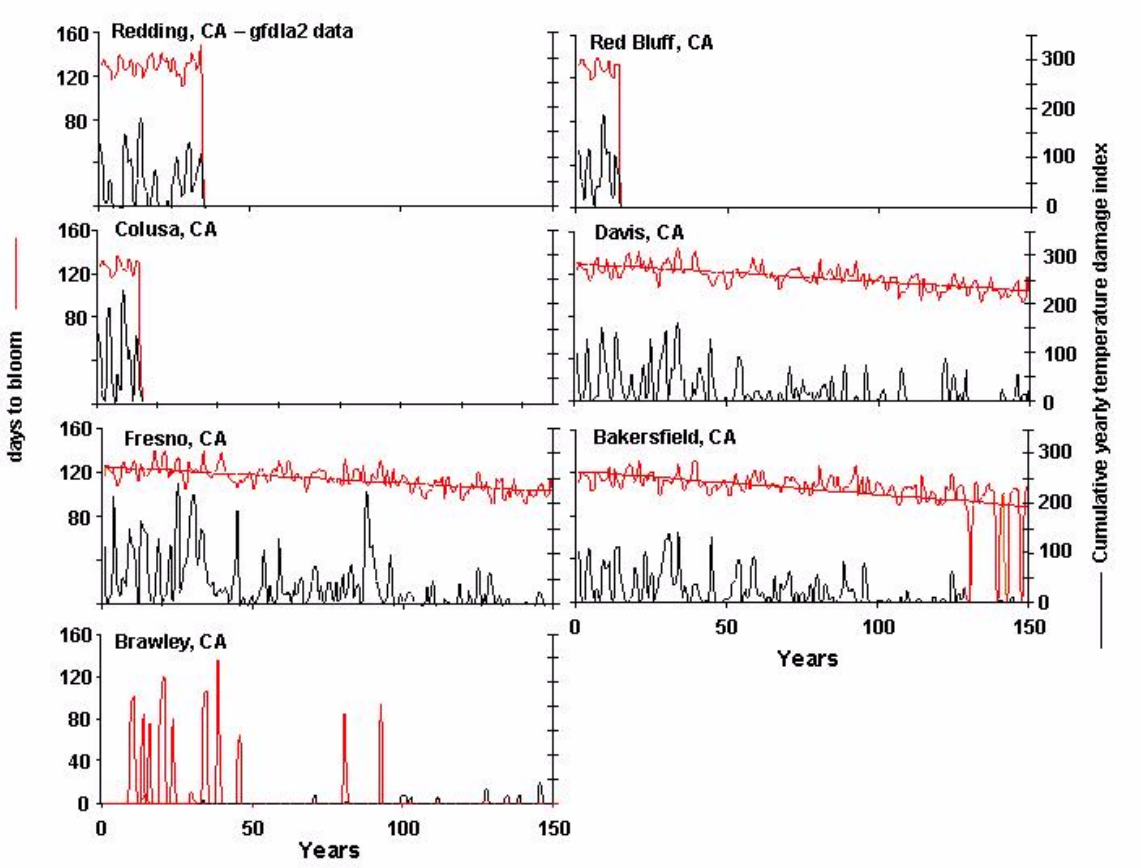

Figure 12. Simulations of olive using the 150-year GFDLA2 weather scenario to predict days to bloom and cumulative temperature damage index at seven locations.

2.4.4. Comparison of weather scenarios at Colusa, California, suppressing the effects of freezing temperatures on olive survival

The goal of this study is to examine whether favorableness for olive culture increases over time with climate change. Hence, the effects of low temperatures that kill trees were suppressed in the model, and the predictions using the four climate warming scenarios for Colusa were compared (Figure 13). Note that only in the original PCMB1 simulations (Figure 9) did the model not predict death of the tree as the result of low temperatures at any of the seven locations.

The time to bloom declines 0.126 days per year and 0.169 days per year in the GFDLB1 and GFDLA2 scenarios, respectively, and 0.080 days and 0.121 days in the PCMB1 and PCMA2 scenarios. The regression intercepts for the four scenarios are essentially the same. The temperature damage indices in the GFDLA2 and PCMA2 scenarios are initially high but decline over the 150-year simulation run, while those in the GFDLB1 and PCMB1 scenarios show less change.

In summary, the decline in time to flowering decreases more in the GFDL scenarios than the PCM scenarios with PCMB1> PCM2A> GFDLB1>GFDLA2.

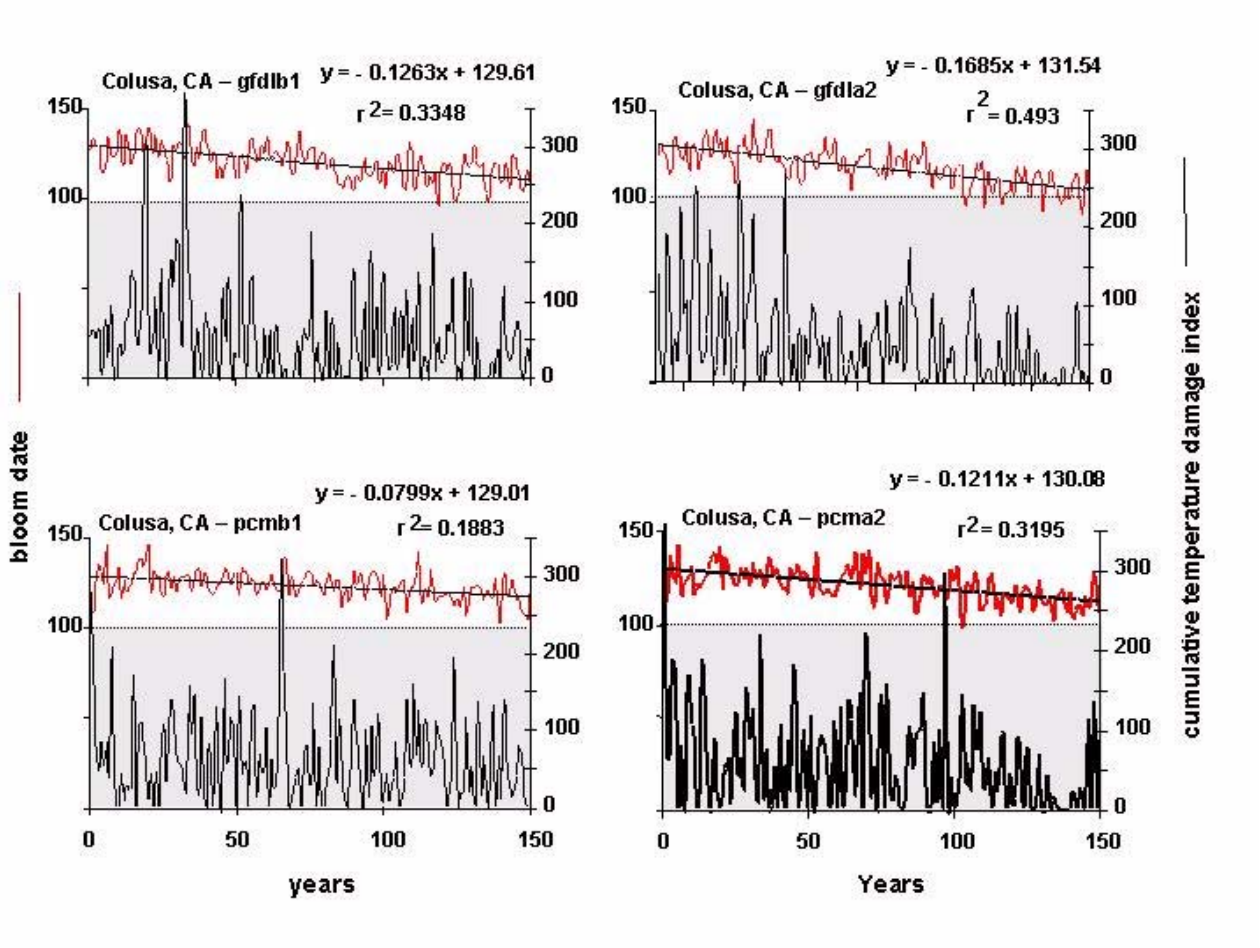

Figure 13. Simulations of olive at Colusa, California, using the four 150-year weather scenarios to predict days to bloom and the cumulative temperature damage index (eqn. 2).

2.5. Yellow Starthistle

Many exotic plants have become important weeds in California agriculture, rangelands and waterways. Yellow starthistle (YST, *Centaurea solstitialis*) is an important rangeland weed that reduces forage quantity and quality, may cause injury to livestock, and is a severe nuisance in recreational areas. The southern distribution of YST in California appears to be limited by soil moisture, and in the central part of its range, currently available biological control agents appear to be ineffective (Gutierrez et al. 2005). Several natural enemies have been introduced to control YST (Figure 14). Among these are two weevils (*Bangasternus orientalis* (*Bo*) and *Eustenopus villosus (Ev)* (Coleoptera: Curculionidae)) and two picture-winged flies (*Urophora sirunaseva (Us)* and *Chaetorellia succinea* (*Cs*) (Diptera: Tephritidae)). These insects attack YST seed heads (capitula), causing variable rates of damage. Simulation of the predicted range and abundance of YST in California (Figure 14), including the impact of natural enemies, accords well with survey data reported by the California Department of Agriculture.

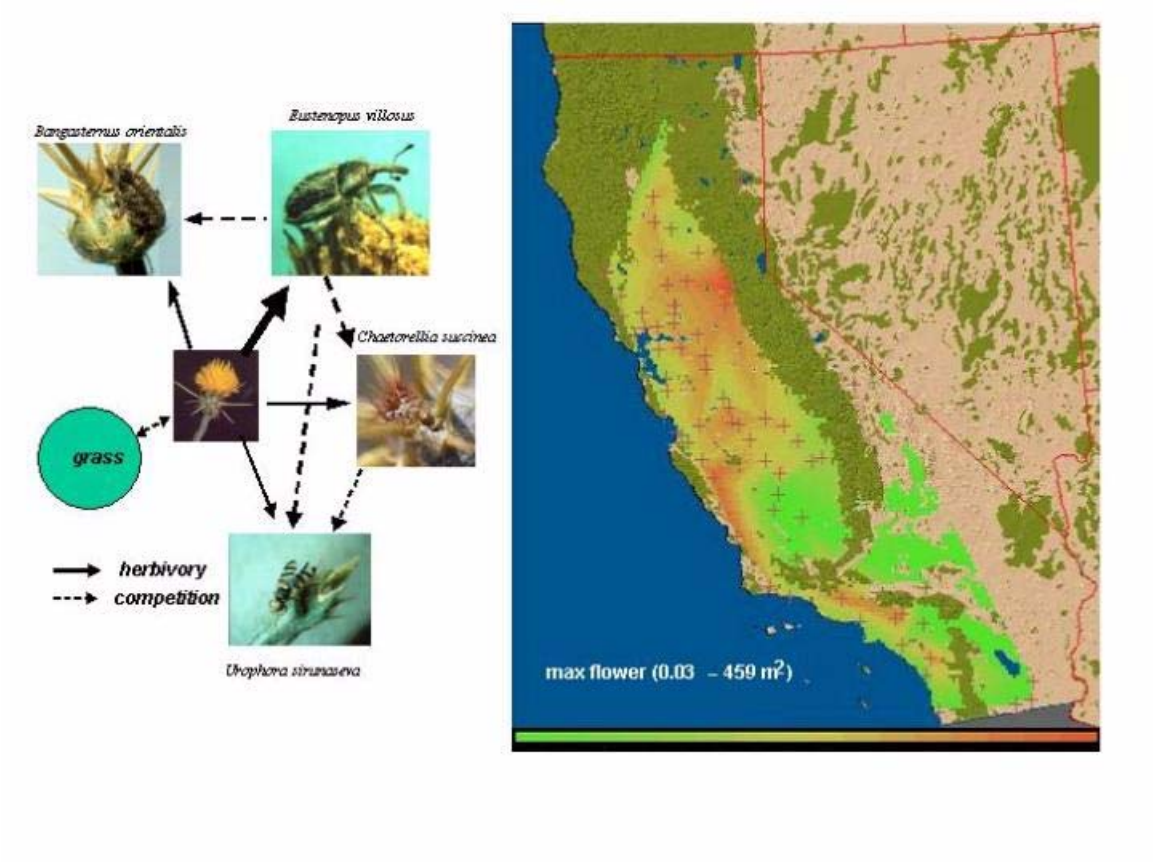

Figure 14. The simulated distribution of yellow starthistle (*Centaurea solstitialis*) flower head densities (capitula) during 2003 in California, given the effects of four introduced natural enemies and competition from annual grasses (cf. Gutierrez et al. 2005).

The regional impact of YST natural enemies was analyzed (Gutierrez et al. 2005) using multiple regression of simulation model output. The natural enemies and competition from annual grasses were included in analysis in all combinations as presence-absence values (i.e., 0 or 1). Only regression coefficients with slopes significantly different from zero were retained in the model.

Marginal analysis of the regression model (i.e., dy/dx_i) suggests that the number of capitula m^{-2} increases with season length (*dd* = degree days > 8°C), cumulative rainfall (*mm*), and *Chaetorellia succinea* (*Cs*) presence, and decreased due to predation by the snout weevil *Eusenopus villosus* (*Ev*) with the interaction *Ev*x*Cs* playing a net minor role.

$$capitula = 171.8 + 0.052dd + 0.16mm - 105.3Ev + 22.3Cs - 29.8Ev \times Cs \quad (3)$$

$$R = 0.53,\ F = 248.6,\ df = 3234$$

Using average values for *dd* (=2,656) and *mm* (=466), average capitula density across the entire region was predicted to remain high (271 per square meter (per m^{-2}).

Equation 4 is the regression model for $\log_{10}$ seed bank density across all sites on season length (*dd*), total rainfall (*mm*), *E. villosus* and *C. succinea*. Natural enemies *B. orientalis* and *U. sirunaseva* were estimated to occur in very low numbers regionwide, and to have little effect in reducing seed pool densities.

$$\log_{10} seed\ density = 3.30 + 0.00007dd + 0.0002mm - 0.18Ev - 0.36Cs + 0.16EvCs \quad (4)$$

$$R = 0.42,\ F = 141.4,\ df = 3234$$

Taking the antilog of eqn. 4 and substituting the mean value for *dd* and *mm* across sites shows that yellow starthistle seed densities increase with season length and total rainfall but decrease with *Ev* and *Cs* presence.

$$seed\ density = 10^{3.3}10^{0.00007\,dd}10^{0.0002\,mm_{rain}}10^{-0.18\,Ev}10^{-0.36\,Cs}10^{0.16\,EvCs} = 1581 \text{ per } m^{-2}$$

where

$10^{3.3} = 1{,}995$ is a constant.

$10^{0.00007\,dd + 0.0002\,mm}$ is the average increase in seed production due to *dd* and rain.

$10^{-0.18\,Ev - 0.36\,Cs + 0.16\text{EvCs}}$ is net survival rates from seed predation.

The combined action of *E. villosus* and *C. succinea* on average reduce seed density 58% across the entire region, with *Cs* having the greatest impact. The impact of *C. succinea* is reduced by its interaction *E. villosus* because the weevil larva kills fly larvae when they co-occur in capitula. The *Ev*x*Cs* interaction increases seed survival 12.8% offsetting much of *Ev's* contribution. Unfortunately, the impact of the natural enemies is insufficient, as it allows more than enough seed to survive to maintain high mature plant populations (i.e., 166 per m^{-2}). Biological control of YST using seed-head feeding insects has so far failed, but the model suggests that natural enemies that attack the whole plant are likely to be better agents.

The effect of climate warming on YST distribution, abundance, and the effectiveness of natural enemies control is explored below.

2.5.1. Comparing the effects of climate warming scenarios GFDLB1 and PCMB1 on YST abundance

Simulation runs made for the seven transect locations included all of the species illustrated in Figure 14. The predicted patterns of abundance of germinating YST plants from the soil seed bank are simulated using site-specific GFDLB1 and PCMB1 climate scenarios. All locations were assume to have the same initial soil seed bank densities (1500 per m^{-2}) the first year of the 150-year runs, but thereafter local production and surviving seed were the initial conditions for subsequent years (see Gutierrez et al. 2005).

PCMB1 scenario - In general, YST seedling densities increased with increasing latitude becoming extremely abundant in the northern part of the range (> 1000 per m^{-2} at Redding; see Figure 15). Densities at Brawley and Bakersfield were low (usually < 20 per m^{-2}), while densities at Fresno were > 100 per m^{-2} and those at Davis and Colusa

were > 300 per m^{-2}. Seedling densities were > 700 per m^{-2} at Red Bluff. In some southern areas, YST seedling densities appear to decrease with time. There is, however, a noticeable increase in YST at Red Bluff after year 85 (roughly 2035) and indications of increases at Redding after year 130 (roughly year 2080).

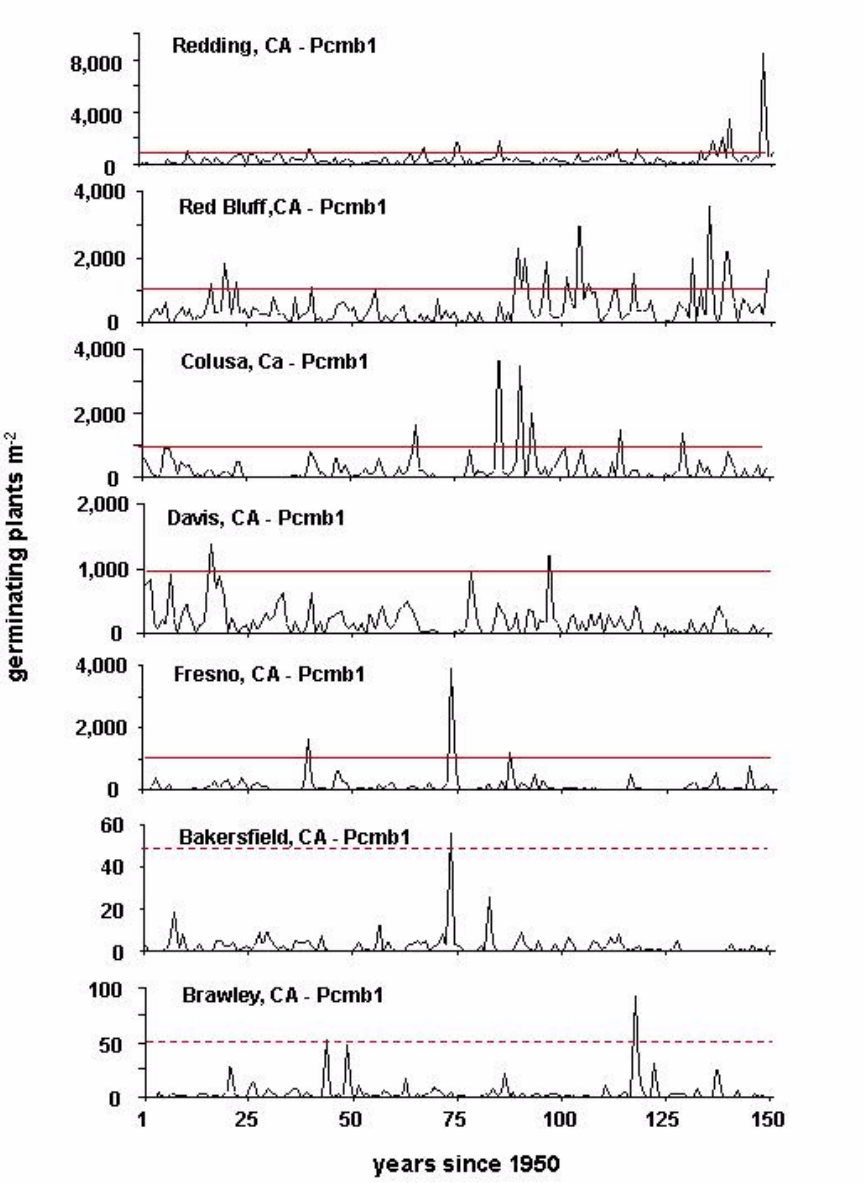

Figure 15. Simulation of yellow starthistle, including the natural enemies illustrated in Figure 14 using the weather scenario PCMB1 at seven locations. Seedling density is used as a measure of YST's potential in the area. The reference lines at 50 and at 1000 are for comparative purposes.

Using the number of mature capitula per m^{-2} as a metric of YST density; and dd, mm, and the density of natural enemy larvae (total larvae per m^{-2}) as independent variables (i.e., $E = Ev$, $U = Us$, $C = Cs$), multiple regression analysis of the YST data using the PCMB1 weather scenario yields the following results.

$$capitula = -178.86 + 0.105\,year - 0.0083dd - 0.197E + 0.033U + 0.033C$$
$$- 0.000025E \times U - 0.000019E \times C - 0.0000037U \times C \qquad (5)$$
$$R^2 = 0.76, \quad df = 1048, \quad F = 422.83$$

Marginal analysis (i.e., dy/dx_i) of eqn. 5 suggests that capitula densities increase on average 0.104 per year, but decrease 0.0083 per degree-day (*dd*). Again, only the snout beetle *E. villosus (E)* reduces seed head densities while the net effect of the two flies (*Urophora sirunaseva (U)* and *Chaetorellia succinea (C)*) result in a net increase due to competition (i.e., the interaction terms). Total rainfall during the season was not significant, nor was herbivory from the other snout beetle *B. orientalis*.

GFDLB1 scenario - YST seedling density generally increases with increasing latitude, again becoming extremely abundant in the northern part of the range (Figure 16). Densities at Brawley and Bakersfield were low and appear to decrease with time (usually < 25 per m^{-2}), while densities at Fresno > 100 per m^{-2} but were intermittently high, while densities at Davis, Colusa, and Red Bluff were usually > 200–300 per m^{-2} but on occasion exceeded 1000 per m^{-2}. At Redding, seedling densities were commonly > 500 per m^{-2} and frequently exceed 1000 per m^{-2}. There is a trend of increasing YST abundance with increasing latitude. No increasing trends are seen over time at any of the locations.

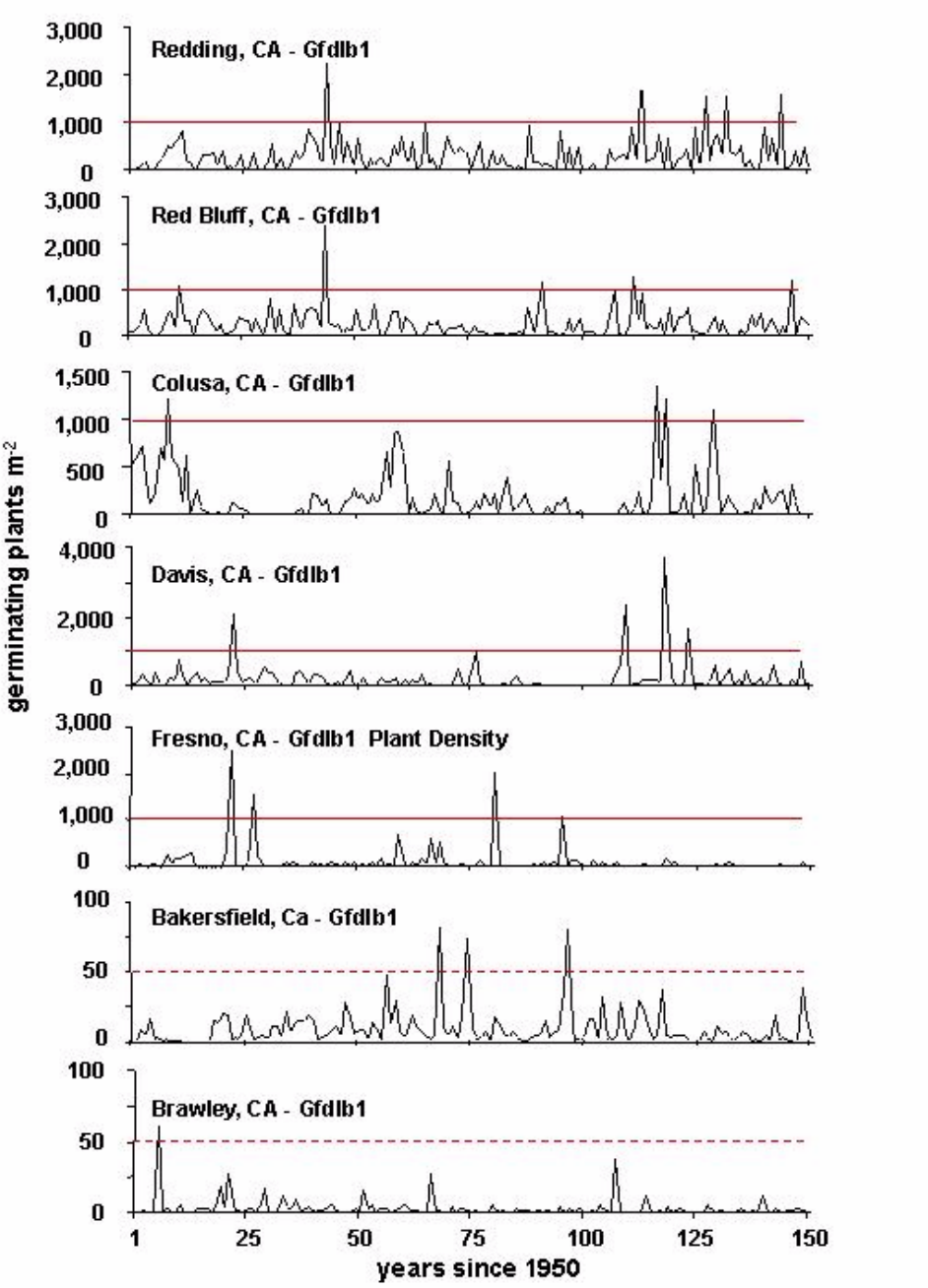

Figure 16. Simulation of yellow starthistle, including the natural enemies illustrated in Figure 14 using the weather scenario GFDLB1 at seven locations. Seedling density is used as a measure of YST's potential in the area. The reference lines at 50 and at 1000 are for comparative purposes.

Using the number of mature capitula per m^{-2} as a metric of YST abundance; and dd, mm, and the density of natural enemy larvae as independent variables (i.e., *E* for *Ev*, *U* for *Us*, *C* for *Cs*), analysis of the YST simulation data using the GFDLB1 climate scenario yields the following.

$$capitula = -211.35 + 0.124\,year - 0.0089\,dd - 0.0924E + 0.027U + 0.041C + 0.000005E \times U - 0.000072E \times C + 0.000006U \times C \quad (6)$$

$$R^2 = 0.65, \quad df = 1048, \quad F = 244.65$$

Marginal analysis (i.e., dy/dx_i) of eqn. 6 suggests that seed head densities increased on average 0.124 per year, but decreased 0.0089 per degree-day (*dd*). Of the natural enemies (*total larvae per m^{-2})*, only the snout beetle *E. villosus (E)* reduced seed head densities, while the net effect of the two flies (*U. sirunaseva (U)* and *C. succinea* (*C*)) resulted in a net increase due to competition. Surprisingly, total rainfall during the season was not significant, nor was herbivory from the snout beetle *B. orientalis*. A separate regression showed that seed head densities also increased with latitude (19 seed heads per m^{-2} per degree).

In summary, under both PCMB1 and GFDLB1 climate change scenarios, YST seedling abundance decreased in the hotter parts of the range and increased in severity northward into colder, formerly less favorable areas (Figures 15 and 16).

3.0 Discussion

That weather is an important factor limiting the potential geographic distribution and abundance of pest and non-pest species is well known. Classic studies of the effects of weather on pest outbreaks are those of locust species in North Africa and the Middle East where they decline to extremely low numbers during periods of drought, but may explode to biblical proportions during prolonged region-wide rainy periods (e.g., Roffey and Popov 1968). In this study, the focus was on the effects of climate change on plant-herbivore – natural enemy interactions, though a similar analysis could have been extended to plant and animal diseases. Some recent analyses of the effects of climate change on arthropod pests range and dynamics include Drake (1994), Ellis et al. (1997), Fleming (1996), and Fleming and Candau (1998). The effects of climate change on the dynamics of diseases of plants and animals were recently reviewed by Coakley et al. (1999). Atmospheric composition (CO_2) also influences susceptibility of crops to pests (e.g., Hamilton et al. 2005) and may increase the severity of invasive weeds (Ziska 2003) and their tolerance to herbicides (Ziska et al. 1999), but these physiological effects could not included in our analysis.

Physiologically based models are becoming increasingly important tools for assessing climate change effects. Gutierrez et al. (1974), Gutierrez and Yaninek (1983), and Hughes and Maywald (1990) used a growth index approach to determine the climatic conditions favorable for the establishment and the development of outbreaks fast reproducing aphids in Australia. Although this approach worked well for the highly migratory cowpea aphid, it would not likely work as well for long-lived pests such as locust across the vast affected areas of North Africa and the Middle East. This is due to the long

period of time required for the outbreaks to develop and the shifting nature of the problem across the landscape. Physiologically based models that capture more of the biology of pests and natural enemies as well as the effects of extant weather on their regional dynamics, provide an excellent mechanism for evaluating such complicated systems (Gutierrez 1996; Schreiber and Gutierrez 1998). The same approach could be used to assess what would happen to the distribution and abundance of crops and pest and non-pest species under different climate change scenarios.

Climate change would complicate the problem of crop production. In this study, a physiologically based model of olive was used to evaluate the effects of climate change scenarios on vernalization and flowering times of olive across the length of California's Great Central Valley. The results suggest that increasing temperatures would decrease olive's range in the southern reaches of the state and cold weather would limit its distribution northward. With global warming, olive production would be consolidated in the central areas of California—the areas of current favorableness. Unlike annual crops that may be easily planted in new areas, long-lived plants such as olive and grape are costly in time and money to reestablish in new locations. Climate change would affect the distribution of the cold-intolerant olive fly.

The effects of weather on pests were recurring in most of our examples, and one can envision the invasion of new areas by pests formerly limited by one or more constraints. The geographic range of the Mediterranean fruit fly (*Ceratitis capitata*) is currently restricted to more southern climes (Messenger and Flitters 1954), but there are incipient medfly populations in southern California (Carey 1996) with occasional infestations and winter dieback in more northern areas. How would climate change affect the distribution and abundance of these and other pests? Likely they would expand northward into current fruit-growing regions.

The range of the cotton pest pink bollworm is limited worldwide by winter frost, hence the predicted milder winters would increase its range northward, say into the San Joaquin Valley of California. Outbreaks of pink bollworm are predicted to be more frequent and severe. The cotton boll weevil is currently limited by desiccation of fruit buds in hot dry areas (DeMichele et al. 1976); hence, if summer rainfall increased, its geographic range within California might also increase. An expansion of the range and abundance in boll weevil occurred during the early 1980s, when a sequence of very wet years in Arizona and Southern California coupled with the cultivation of stub-cotton temporarily increased favorableness in the region, but subsided as drier weather returned. How many other pest species will be similarly affected is at present unknown, and will require analysis.

Pest regulation by natural enemies (i.e., biological control) would similarly be affected. Examples abound in the literature in such diverse crops as alfalfa, citrus, grape, and the weed yellow starthistle. Control of YST by plant feeding natural enemies has been checkered because their damage is insufficient to prevent plant compensation and each has it own climatic requirements that limit the geographic range. In general, biological control of YST has been poor in California, but an analysis by Gutierrez et al. (2005) suggests that natural enemies that attack the whole plant and reduce its capacity to produce seed and to compensate for competition and damage would be better

candidates for introduction. Examples of such natural enemies are a pathogenic fungus specific to YST that is currently being released in California. Another possible candidate is a host-specific insect species that damages the root system. This natural enemy is being evaluated for introduction by the United States Department of Agriculture (USDA) in Albany, California, and the California Department of Food and Agriculture (CDFA). Better control of YST has been reported in Oregon, where the shorter growing season reduces YST's capacity to compensate for herbivore damage, but our analysis suggests that this would change with global warming. The analysis predicts that YST would increase in severity in more northern regions. Because of the tremendous losses accruing to California agriculture from exotic insect pests and weeds and the generally cost effectiveness of biological control, additional support for biological control would be warranted.

Assessing the impact of climate warming on crop pest-natural enemy interactions is difficult and requires simplified but realistic models to examine these issues. The current limitation to implementing a physiologically based modeling approach is the lack of infrastructure for collecting the requisite biological data for developing, refining and testing such models. The availability of appropriate weather data to implement the models and to project their results on a large geographic scale is also lacking. The cost to correct these deficiencies is relatively small, while the potential benefits are large. The development of such system models for the major crops in California was a major goal, now abandoned, of the UC/IPM Statewide Program when it was first started in 1978. Greater emphasis should be placed on developing these models.

4.0 References

Bieri, M., J. Baumgärtner, G. Bianchi, V. Delucchi, and R. Von Arx. 1983. "Development and fecundity of pea aphid (*Acyrthosiphon pisum* Harris) as affected by constant temperatures and pea varieties." *Mitt. Schweiz. Entomol. Ges.* 56:163–171.

Campbell, A., B. D. Frazer, N. Gilbert, A. P. Gutierrez, and M. Mackauer. 1974. "Temperature requirements of some aphids and their parasites." *J. Appl. Ecol.* 11: 431–438.

Carey, J. R. 1996. "The incipient Mediterranean fruit fly population in California: implications for invasion biology." *Ecology* **77** (1996), 1690–1697.

Coakley S. M., H. Scherm, and S. Chakraborty. 1999. "Climate change and plant disease management." *Annual Rev Phytopath* 37: 399-426.

Dalla Marta, A., S. Orlandini, P. Sacchetti, and A. Belcari. 2004. "*Olea europaea*: integration of GIS and simulation modeling to define a map of "dacic attack risk" in Tuscany." *Adv. Hort. Sci.* 18(4):168–172.

DeBach, P. 1964. *Biological control of Insect Pests and Weeds*. Chapman and Hall, London, 844.

DeBach, P., and R. A. Sundby. 1963. Competitive displacement between ecological homologues. *Hilgardia* 34:105–166.

DeMelo-Abreu, D. Barranco, A. M. Cordiero, J. Tous, B. M. Rogado, and F. J. Villalobos. 2004. "Modelling olive flowering date using chilling for dormancy release and thermal time." *Agric. For. Meteorology* 125:117–127.

DeMichele, D. W., G. L. Curry, P. J. H. Sharpe, and C. S. Barfield. 1976. "Cotton bud drying: A theoretical model." *Environ. Entomol.* 5:1011–1016.

Denney, J. O., and G. R. McEachern. 1985. "Modeling the thermal adaptability of the olive (*Olea europaea* L.) in Texas." *Agric. For. Meteorology* 35:309–327.

DiCola, G., G. Gilioli, and J. Baumgärtner. 1999. Mathematical models for age-structured population dynamics. In *Ecological Entomology*, (C. B. Huffaker and A. P. Gutierrez, editors, second edition) John Wiley and Sons. New York. 503–534.

Drake, V. A. 1994. "The influence of weather and climate on agriculturally important insects: An Australian perspective." *Aust. J. Agric. Res.* 45: 487–509.

Ellis, W. N., J. H. Donner, and J. H. Kuchlein. 1997. "Recent shifts in phenology of Microlepidoptera, related to climatic change Lepidoptera)." *Entomol. Berichten* (Amsterdam) 57: 66–72.

Fleming, R. A. 1996. "A mechanistic perspective of possible influences of climate change on defoliating insects in North America's boreal forests." *Silva Fennica* 30: 281–294.

Fleming, R. A., and J-N. Candau. 1998. "Influences of climatic change on some ecological processes of an insect outbreak system in Canada's boreal forests and the implications for biodiversity." *Environ. Monitoring and Assessment* 49:235–249.

Fitzpatrick, E. A., and H. A. Nix. 1970. The climatic factor in Australian grasslands ecology. In *Australian Grasslands* (Ed. R. M. Moore). Australian National University Press. 3–26.

Gilbert, N. E., and A. P. Gutierrez. 1973. "A plant-aphid-parasite relationship." *J. Anim. Ecol.* (42): 323–340.

Gilbert, N., A. P. Gutierrez, B. D. Frazer, and R. E. Jones. 1976. *Ecological Relationships*. Freeman and Co., New York.

Gutierrez, A. P. 1992. The physiological basis of ratio dependent theory. *Ecology* 73: 1552–63.

Gutierrez, A. P. 1996. *Applied Population Ecology: A supply-demand approach*. John Wiley and Sons, New York. 300 pp.

Gutierrez, A. P., 2001. Climate Change: Effects on Pest Dynamics. In *Climate Change and Global Crop Productivity*, K. R. Reddy and H. F. Hodges, editors. London: CAB International.

Gutierrez, A. P., and J. U. Baumgärtner. 1984. "Multitrophic level models of predator-prey-energetics: I. Age specific energetics models-pea aphid *Acyrthosiphon pisum* (Harris) (Homoptera: Aphididae) as an example." *Can. Ent.* 116: 924–932.

Gutierrez, A. P., and K. Daane. 2005. UC/IPM Progress Report.

Gutierrez, A. P., G. D. Butler, Jr., Y. Wang, and D. Westphal. 1977. "The interaction of the pink bollworm, cotton and weather." *Can. Entomol.* 109: 1457–1468.

Gutierrez, A. P., C. K. Ellis, and R. Ghezelbash. "Climatic limits of pink bollworm in Arizona and California: Effects of climate warming." (submitted) *Acta Oecologica* (in press).

Gutierrez, A. P., L. A. Falcon, W. B. Loew, P. Leipzig, and R. van den Bosch. 1975. "An analysis of cotton production in California: A model for Acala cotton and the efficiency of defoliators on its yields." *Env. Ent.* 4(1): 125–136.

Gutierrez, A. P., D. E. Havenstein, H. A. Nix, and P. A. Moore. 1974. "The ecology of *Aphis craccivora* Koch and subterranean clover stunt virus. III. A regional perspective of the phenology and migration of the cowpea aphid." *J. Appl. Ecol.* 11: 21–35.

Gutierrez, A. P., S. J. Mills, S. J. Schreiber, and C. K. Ellis. 1994. "A physiologically based tritrophic perspective on bottom up - top down regulation of populations. *Ecology* 75: 2227–2242.

Gutierrez, A. P., P. Neuenschwander, F. Schulthess, H. R. Herren, J. U. Baumgärtner, B. Wermelinger, J. S. Yaninek, and C. K. Ellis. 1988. "Analysis of biological control of cassava pests in Africa: II. Cassava mealybug, *Phenacoccus manihoti*." *J. Appl. Ecol.* 25: 921–940.

Gutierrez, A. P., M. J. Pitcairn, C. K. Ellis, N. Carruthers, R. Ghezelbash. 2005. "Evaluating biological control of yellow starthistle (*Centaurea solstitialis*) in California: A GIS based supply–demand demographic model." *Biological Control* 34: 115–131.

Gutierrez, A. P., B. Wermelinger, F. Schulthess, J. U. Baumgärtner, H. R. Herren, C. K. Ellis, and J. S. Yaninek. 1988. "Analysis of biological control of cassava pests in Africa: I. Simulation of carbon nitrogen and water dynamics in cassava." *J. Appl. Ecol.* 25: 901–920.

Gutierrez, A. P., and J. S. Yaninek. 1983. "Responses to weather of eight aphid species commonly found in pastures in southeastern Australia." *Can. Ent.* 115: 1359–1364.

Hamilton, J. G., O. Dermody, M. Aldea, A. R. Zangerl, A. Rogers, M.R. Berenbaum, and E. H. Delucia. 2005. "Anthropogenic changes in tropospheric composition increase susceptibility of soybean to insect herbivory." *Environ Entomology* 34(2): 479–455.

Hartmann, H. T., and K. W. Opitz. 1980. Olive production in California, rev. ed. Leaflet 2474, University of California Div. Agric. Sci., Davis, California.

Hayhoe, K., D. Cayan, C. Field, P. Frumhoff, E. Maurer, N. Miller, S. Moser, S. Schneider, K. Cahill, E. Cleland, L. Dale, R. Drapek, R. M. Hanemann, L. Kalkstein, J. Lenihan, C. Lunch, R. Neilson, S. Sheridan, and J. Verville, 2004. Emissions pathways, climate change, and impacts on California. Proceedings of the National Academy of Sciences (PNAS) 101 (34): 12422–12427.

Hughes, R. D., and G. W. Maywald. 1990. "Forecasting the favorableness of the Australian environment for the Russian wheat aphid, *Diuraphis noxia* (Homoptera: Aphididae), and its potential impact on Australian wheat yields." *Bull. Entomol. Res.* 80: 165–175.

Mancuso, S., G. Pasquili, and P. Fiorino. 2002. "Phenology modelling and forecasting in olive (*Olea europaea* L.) using artificial neural networks." *Adv. Hort. Sci.* 16(3–4):155–164.

Maurer, E. P. 2005. "Uncertainty in hydrologic impacts of climate change in the Sierra Nevada Mountains, California under two emissions scenarios." *Climatic Change* (submitted 29 April 2005).

Maurer, E. P., and P.B. Duffy. 2005. "Uncertainty in projections of stream flow changes due to climate change in California." *Geophys. Res. Let.* 32(3), L03704 doi:10.1029/2004GL021462.

Messenger, P. S. 1964. "Use of life-tables in a bioclimatic study of an experimental aphid-braconid wasp host-parasite system." *Ecology* 45: 119–131.

Messenger, P. S. 1968. "Bioclimatic studies of the aphid parasite *Praon exsoletum*. 1. effects of temperature on the functional response of females to varying host densities." *Can. Ent.* 100: 728–741.

Messenger, P. S., and N. E. Flitters. 1954. "Bioclimatic studies of three species of fruit flies in Hawaii." *J. Econ. Entomol.* 47:756–765.

Nechols, J. R., M. J. Tauber, C. A. Tauber, and S. Masaki. 1998. Adaptations to Hazardous Seasonal Conditions: Dormancy, Migration, and Polyphenism. In *Ecological Entomology*, C. B. Huffaker and A. P. Gutierrez (eds.). New York: John Wiley and Sons.

Pickering, J., and A. P. Gutierrez. 1991. "Differential impact of the pathogen *Pandora neoaphidis* (R. & H.) Humber (Zygomycetes: Entomophthorales) on the species composition of *Acyrthosiphon* aphids in alfalfa." *Can. Ent.* 123: 315–320.

Pimentel, D., L. Lach, R. Zunig, and D. Morrison. 2000. "Environmental and economic costs of nonindigenous species in the United States." *BioScience* 50: 53–65.

Quezada, J. R., and P. DeBach. 1973. "Bioecological and population studies of the cottony scale, *Icerya purchasi* Mask., and its natural enemies. *Rodolia cardinalis* Mul. And *Cryptochaetum iceryae* Wil., in southern California." *Hilgardia* 41:631–688.

Reddy, K. R., and H. F. Hodges (editors). 2001. *Climate Change and Global Crop Productivity*. London: CAB International.

Rochat, J. and A. P. Gutierrez (2001) Weather mediated regulation of olive scale by two parasitoids. J. Anim. Ecol. 70: 476–490.

Roffey J. and G. Popov. 1968. Environmental and behavioural processes in Desert locust outbreaks. Nature 219: 446–450.

Schreiber, S. and A. P. Gutierrez. 1998. A supply-demand perspective of species invasions and coexistence: applications to biological control. Ecol. Modelling 106: 27–45.

Shelford, V. E. 1931. Some concepts of bioecology. Ecology 12: 455–467.

Sutherst, R. W., G. F. Maywald and W. Bottomly. 1991. From CLIMEX to PESKY, a generic expert system for risk assessment. *EPPO Bulletin* 21: 595–608.

Vansickle, J. 1977. Attrition in distributed delay models. *IEEE Trans. Sys., Man. Cybern*. 7: 635–638.

Venette, R. C., S. E. Naranjo, W. D. Hutchison. 2000. "Implications of larval mortality at low temperatures and high soil moistures for establishment of pink bollworm (Lepidoptera: Gelechiidae) in Southeastern United States cotton." *Environ. Entomol.* 29(5): 1018–1026.

von Liebig, J. 1840. *Chemistry and its Applications to Agriculture and Physiology*. London, Taylor and Walton. (4th edition 1847).

Walther G. R. 2002. "Ecological responses to recent climate change." *Nature* 416: 389–395.

Watt, K. E. F. 1959. "A mathematical model for the effects of densities of attacked and attacking species on the number attacked." *Can. Entomol.* 91: 129–144.

Wit de, C. T., and J. Goudriaan. 1978. *Simulation of Ecological Processes.* 2nd edit. The Netherlands: PUDOC Publishers.

Ziska L. H. 2003. "Evaluation of growth response of six invasive species to past, present, and future atmospheric CO_2." *J. Exp Botany* 54(389): 395–406.

Ziska, L. H., J. R. Teasdale, J. A. Bunce. 1999. "Future atmospheric CO_2 may increase tolerance to glyphosate." *Weed Sci.* 47:608–615.

Appendix A

A Weather-driven Tritrophic Model

A plant-herbivore (and higher tropic levels) model may be viewed as *ns* {n = 1, ns} linked *functional* age/mass structured population models. The plant is a canopy model consisting of five linked demographic models: mass of leaves {n = 1}, stem {2} and root {3}, and for fruit mass and numbers {4, 5}. These models {1–5} are linked by photosynthate production and allocation with the ratio of production to demand controlling all vital rates (cf. Gutierrez, Neuenschwander et al. 1988 and Gutierrez, Wermelinger et al. 1988). The age-structured number dynamics of herbivore is modeled using a similar model {6} linked to plant fruit models {4, 5} that it uses as hosts for its progeny.

Each of the *functional* populations may be modeled using a time-invariant distributed-maturation time age-structure model (eqn. A1, Vansickle 1977, see DiCola et al. 1999 for related model forms). We use the notation of DiCola et al. (1999, p 523–524) to describe the Vansickle (1977) distributed maturation time model used in our analysis. This model is characterized by assumption

$$v_i(t) = v(t) = \frac{k}{del(t)}\Delta a \qquad i=0,1,\ldots,k \tag{A1.1}$$

where k is the number of age intervals, $del(t)$ is the expected value of emergence time and Δa is an increment in age. From (A1.1) we obtain

$$\frac{dN_i}{dt} = \frac{k}{del(t)}[N_{i-1}(t) - N_i(t)] - \mu_i(t)N_i(t) \tag{A1.2}$$

where N_i is the density in the ith cohort and $\mu_i(t)$ is the proportional net loss rate. In terms of flux $r_i(t) = N_i(t)v_i(t)$, yields

$$\frac{d}{dt}\left[\frac{del(t)}{k}r_i(t)\right] = r_{i-1}(t) - r_i(t)] - \frac{del(t)}{k}\mu_i(t)r_i(t)\,. \tag{A1.3}$$

The model is implemented in discrete form (see Gutierrez 1996).

Aging occurs via flow rates $r_{i-1}(t)$ from N_{i-1} to N_i, births enter the first age class of the population, deaths at maximum age exit the last or k^{th} age class, and net age-specific proportional mortality (losses and gains) from all factors is included

in $-\infty < \mu_i(t) < +\infty$. The mean developmental time of a population is v with variance V with the age width of an age class being v/k and $k = v^2/V$. The number of individuals (or mass units) in age class i is $N_i(t) = r_i(t)v/k$, and that in the total population is $N(t) = \sum_{i=1}^{k} N_i(t) = \frac{v(t)}{k}\sum_{i=1}^{k} r_i(t)$. If k is small, the variability of developmental times is large and *vice-versa*. A value of k =45 was chosen to produce a roughly normal distribution of developmental times.

The developmental time of herbivore larvae varies with fruit host age, and both the host and the larvae age on their own temperature-time scale (see below). Hence larvae initially infesting specific age fruits at time t will in the course of their development experience changing host characteristics that affect their developmental times, mortality and potential fecundity as an adult. To handle this biology, a two-dimensional time-invariant distributed maturation time model with flows in the fruit age and age of pest dimensions is utilized (eqn. A2).

$$\frac{dN_{i,j}}{dt} = \frac{k}{del(t)}[N_{i-1,j-1}(t) - N_{i,j}(t)] - \mu_{i,j}(t)N_{i,j}(t) \qquad \text{(A2)}$$

The mean developmental rate of a cohort of larvae ($v(t,i,j)$) is transient and depends on host fruit age. Hence, if i is larval age and j is its host fruit age, the model is updated for flow first in the i^{th} and then the j^{th} dimension taking care to correct for differences in developmental time scales between cells. For convenience, the net proportional mortality term $\mu_{nij}(t)N_{i,j}$ is applied in the i^{th} dimension and assumed zero in the j^{th} dimension. This scheme also allows mortality to herbivore eggs and larvae due to fruit subunit shedding to be applied to larvae in each *i,j* cohort. herbivore population density.

$$N(t) = \sum_{j=1}^{k}\sum_{i=1}^{k} N_{nij}(t) = \sum_{j=1}^{k}\frac{v(t,j)}{k}\sum_{i=1}^{k} r_{nij}(t)\,. \qquad \text{(A3)}$$

Physiological time and age

Plant and its pests are poikilotherms and hence time and age in the model are in physiological time units. The linear degree-day model (A4) was used to model the temperature (T) dependent development rate ($\Delta v(t(T))$ because sufficient data across the full range of temperatures was unavailable.

$$\Delta v(t(T)) = \frac{1}{v(t(T))} = c_1 + c_2 T(t) \qquad \text{(A4)}$$

Constants c_1 and c_2 are fitted to species data. The lower developmental threshold ($\Delta v(t(T)) = 0$) for the plant and herbivore (and higher trophic levels) may differ. A time step in the model is a day of varying physiological time (degree days d^{-1} = Δdd) computed above appropriate threshold using the half sine method (Gilbert and Gutierrez 1973; Campbell et al. 1974).

Growth rates

As rates, per capita resource acquisition ($S(u)$) is allocated in priority order to egestion (β) respiration (i.e., Q_{10}), costs of conversion (λ) and to reproductive and growth rates (GR).

$$GR(t) = \phi^*(t)(S(u)\beta - Q_{10})\lambda \qquad \text{(A5.1)}$$

The realized GR must also include the effects of other limiting factors. This is done by the scalar (ϕ^*) that is the product of the daily supply-demand ratios for the other essential resources (see eqn. 1 and below). Resource acquisition $S(u)$) involves search and depends on the organism's maximum assimilative capacity (i.e., its demand, $D(u)$). This quantity may be estimated experimentally under conditions of non-limiting resource.

$$D(u) \approx S(U) = (GR_{\max}(t)/\lambda + Q_{10})/\beta . \qquad \text{A(5.2)}$$

Resource acquisition - Plants capture light, water and inorganic nutrients and herbivore larvae attack plant subunits (e.g., fruit). The biology of resource acquisition by a population of plant or animal consumers ($N(t)$) involves search under conditions of time

varying resource (*R(t)*). The maximal population demand is *D=D(u)N*. Resource acquisition (*S*) is modeled using the ratio-dependent Gutierrez and Baumgärtner (1984) functional response model (eqn. A6, Gutierrez, 1992) that is a special case of Watt's model (1959) because it includes eqn. 5.2 (see Gutierrez 1996 (p. 81) for the derivation of this model). We simplify the notation as follows.

$$S = Dh(u) = D\left[1 - \exp\left(\frac{-\alpha R}{D}\right)\right]. \qquad \text{(A6)}$$

h(u) is the proportion of the resource demand (*D,* eqn. 5.2) that was obtained and α is the search parameter. α may also be a convex function of *N* making (A6) a type III functional response (Rochat and Gutierrez 2001; (i.e., $\alpha = 1 - \exp(-sN)$) with search constant *s*)). As a function of *N*, α for plants becomes Beer's Law and for animals it is the Nicholson-Bailey model. Note that intra-specific competition enters the model via the ratio of available resource to population demand ($\frac{-\alpha R}{D}$). Note also that inter-specific competition also enters in this manner.

The resource (R) for plant is the light energy (cal $m^{-2}d^{-1}$) per unit of ground at time *t* multiplied by a constant that converts it to g dry matter $m^{-2}d^{-1}$. For herbivore, *R* may be the sum of all age fruit (or leaves, age=*j*) corrected for preference ($0 \le \xi_j \le 1$).

$$R = \sum_{j=1}^{J} \xi_j R_j \qquad \text{(A7)}$$

Note that stages with preference values equal to zero are effectively removed from the calculations.

The total age specific consumer demand (*D*) across ages (*i= 1, k*) may be computed in mass or number units as appropriate for the population.

$$D = \sum_{i=1}^{k} D_i^* N_i \qquad \text{(A8)}$$

In plant, the demand rate (g dry matter d^{-1}) is the sum of all subunit population maximum demands corrected for the costs of conversion of resource to self and respiration (eqn. A5.2, see Gutierrez and Baumgartner 1984).

In pests such as herbivore, the demand rate is the maximum per capita adult demand for oviposition sites and is computed using eqn. A9.

$$D^{*}_{i=a} = \theta\phi_T(T)f(a) \qquad \text{(A9)}$$

$f(a) = \frac{ca}{d^a}$ is the maximum age (a) specific per capita fecundity at the optimum temperature with parameters c and d (cf Bieri et al., 1983).

$\theta = 0.5$ is the sex ratio.

$\phi_T(T)$ is the correction for the effect of temperature dependent respiration.

Supply-demand effects - Consumer resource acquisition success is estimated by the acquisition supply/demand ratio ($\phi_{S/D}(t)$) obtained by dividing both side of eqn. A6 by the population demand D.

$$0 \le \phi_{S/D}(t) = S/D = h(u) < 1 \cdot \qquad \text{(A10)}$$

Some consumers may have multiple resources and they must be included in the computation (see below).

In plant, success in meeting its demand is measured by the photosynthate *supply/demand* ratio (e.g., $0 \le \phi_{\cot,S/D} < 1$) but there may be shortfalls of water (w) and inorganic nutrients (η) that may also computed using variants of (eqn. A6). For example, the water $0 \le \phi_w = S_w/D_w < 1$ ratio is computed in three steps: (i) the potential evapo-transpiration ($D_w = PET$) and evaporation from the soil surface (ES) are estimated using a Penman based biophysical model; (ii) D_w along with available soil water in the root zone ($w = W_{max} - W_{wp}$) above the wilting point (w_{wp}) are substituted in eqn. A6 to compute evapo-transpiration ($S_w = ET$, i.e., water use by the plant); and (iii) the input-output model balances rainfall (*rain*, *ES*, *ET)* and runoff or flow through above maximum soil water holding capacity (W_{max}) (see Gutierrez, Wermelinger et al. 1988).

$$w_{WP} \le w(t+1) = w(t) + rain(t) - ES(t) - ET(t) \le W_{\max} \quad \text{(A11)}$$

Similarly for nitrogen, $0 \le \phi_\eta = S_\eta / D_\eta < 1$ is computed using analogues of eqns. A6-A 8 and A10 (see Gutierrez, Wermelinger et al. 1988 for details).

The combined effect of shortfall of all essential resources is captured as the product of the independent supply-demand ratios (eqn. A12) (i.e., survivorship terms, Gutierrez et al. 1994).

$$0 \le \phi^* = \phi_{(S/D)} \phi_{(w)} \phi_{(\eta)} \ldots < 1. \quad \text{(A12)}$$

Eqn. A12 is functionally von Liebig's Law of the Minimum because if any component of ϕ^* causes the supply to fall below a limiting value (e.g., respiration in plant, see A6), it becomes the limiting factor. In plants, after respiration and conversion costs have been subtracted from $\phi^* D$, the remaining photosynthate is allocated in priority order to meet demands for reproduction and then vegetative growth and reserves (see Gutierrez 1992, 1996). In addition to slowing the growth rates of subunits, ϕ^* also reduces the production rate of new subunits, the survival of extant ones (e.g., fruit shedding), and in the extreme may causes the death of the whole plants.

Say individual herbivore larvae infest individual fruit making their behavior more akin to that of a parasitoid. For this reason, the effects of temperature on respiration and hence fecundity are introduced in an approximate way. In poikilotherms, respiration increases with temperature and a plot of the net assimilation rate (supply – respiration) on temperature typically yields a humped or concave function over the range favorable for development with zero values occurring at the lower and upper thermal thresholds and the maximum assimilation rate occurs at T_{opt}. This function is similar to that in CLIMEX but arises naturally in our plant model. However, to capture the effect of temperature on herbivore fecundity, we assume that the normalized effect of temperature on fecundity (i.e., the physiological index for temperature, $0 \le \phi_T(t) \le 1$) is similarly convex (see Gutierrez et al. 1994; Rochat and Gutierrez 2001). The simplest form for ϕ_T is convex symmetrical (eqn. A13).

$$\phi_T = \begin{cases} 1 - \left(\dfrac{(T - T_{\min}) - \gamma}{\gamma} \right)^2 & \text{if } T_{\min} \le T \le T_{\max} \\ \text{otherwise} \quad 0 \end{cases} \tag{A13}$$

The temperature thresholds for development are $T_{\min}$ and $T_{\max}$, and $\gamma = T_{\max} - T_{\min}) / 2$ is half the favorable range and $T_{opt} = (T_{\max} + T_{\min}) / 2$ is the midpoint.